THERMO-PHYSICAL MODELING OF POWDER MIXED NEAR DRY ELECTRICAL DISCHARGE MACHINING PROCESS

A DISSERTATION

SUBMITTED IN PARTIAL FULFILLMENT OF THE REQUIREMENTS

FOR THE AWARD OF THE DEGREE

OF

MASTER OF TECHNOLOGY

IN

[**PRODUCTION ENGINEERING**]

Submitted by :

[**JITENDRA YADAV**]

(**Roll No. 2K16/PIE/009**)

Under the supervision of

Prof. R.S.Walia **Prof. Rajesh Kumar**

DEPARTMENT OF MECHANICAL ENGINEERING
DELHI TECHNOLOGICAL UNIVERSITY
(Formerly Delhi College of Engineering)
Bawana Road, Delhi-110042

JULY, 2018

CANDIDATE'S DECLARATION

I, JITENDRA YADAV, 2K16/PIE/009 student of M.Tech, PRODUCTION ENGINEERING hereby declare that the project Dissertation titled "**THERMO-PHYSICAL MODELING OF POWDER MIXED NEAR DRY ELECTRICAL DISCHARGE MACHINING PROCESS**", which is submitted to the **Department of MECHANICAL ENGINEERING**, Delhi Technological University, Delhi in partial fulfilment of the requirement for the award of degree of Master of Technology, is original and not copied from any source without proper citation. This work has not previously formed the basis for the award of any Degree, Diploma Associateship, Fellowship or other similar title or recognition.

Place : Delhi

Date:

JITENDRA YADAV

2K16/PIE/009

M.Tech (PIE)

CERTIFICATE

I hereby certify that the Project Dissertation titled "**THERMO-PHYSICAL MODELING OF POWDER MIXED NEAR DRY ELECTRICAL DISCHARGE MACHINING PROCESS**" which is submitted by **Mr. JITENDRA YADAV**, **2K16/PIE/009, Mechanical Engineering,** Delhi Technological University, Delhi in partial fulfilment of the requirement for the award of the degree of Master of Technology, is a record of the project work carried out by the student under my supervision. To the best of my knowledge this work has not been submitted in part or full for any Degree or Diploma to this university or elsewhere.

Supervisor
Dr. R.S.WALIA
(**Professor**)

Supervisor
DR. RAJESH KUMAR
(Professor)

Place: Delhi

Date:

ACKNOWLEDGEMENT

It is a matter of great pleasure for me to present my major project report on "**THERMO - PHYSICAL MODELING OF POWDER MIXED NEAR DRY ELECTRICAL DISCHARGE MACHINING PROCESS**". First and foremost, I am profoundly grateful to my guide **Dr. R.S.Walia, Professor, Mechanical Engineering Department, DTU** and supervisor **Dr. Rajesh Kumar, Professor, Mechanical Engineering Department, DTU** for their expert guidance and continuous encouragement during all stages of report. I feel lucky to have an opportunity to work with them. Not only their understanding towards the subject, but also their interpretation of the results drawn from the graphs were very thought provoking. I am thankful to the kindness and generosity shown by them towards me, as it helped me morally in completing the project before actually starting it.

I would like to thank, **Mr. Sanjay Sundriyal** (PhD. Scholar) for all his assistance during execution of this project work, without his support it would be almost impossible to complete my work on time.

Place: Delhi JITENDRAYADAV

Date: (2K16/PIE/09)

ABSTRACT

Electric discharge machining (EDM) is a widely used non-traditional machining process used in the manufacturing of complex shaped dies, molds, parts used in automobile, aerospace, surgical and other industrial components. The process uses thermal energy of the spark to machine electrically conductive material regardless of their hardness and brittleness. This unique feature of EDM has a distinct advantage in the manufacture of complex shaped die and molds made up of hard materials which are difficult to machine by conventional machining processes.

Near dry electric discharge machining (ND-EDM) is advanced method of EDM which is eco-friendly and also more efficient in terms of material removal rate than traditional EDM. In this research an approach has been made to perform a hybrid electrical discharge machining operation on EN-31 steel which utilizes metallic powder as an additive along with dielectric such as air in ND-EDM. This hybrid method of machining is known as Powder mixed near dry EDM (PMND-EDM). This study involves modelling for output process parameter i.e. MRR. The experiments were performed and comparative study has been done between the results obtained by modelling and experiments. The peculiarity of this work is the provision of break down timing in the calculation of heat flux. Moreover, the inclusion of critical concentration ratio into the expression of break-down time provides direct relationship of powder concentration level in the multiphase dielectric mixture with the break down time. It was concluded that the modelling has been done successfully and results obtained do comply with the methodology of the research.

CONTENTS

LIST OF FIGURES

LIST OF TABLES

LIST OF SYMBOLS, ABBREIVATIONS AND NOMENCLATURE

Symbol	Description
F_c	Heat distribution factor
V_b	Break down voltage (Volts)
V_o	Supply voltage(Volts)
V_o	Voltage reached inside the capacitor(Volts)
$\mathcal{R}_c$	Charging Resistance (ohm)
ς	Capacitance of condenser (F)
ξ_c	Energy delivered to discharging circuit(J)
$\mathfrak{I}$	time constant (s)
$\mathfrak{I}_c$	time constant value at maximum power condition(s)
H_{mean}	Mean heat delivered within the circuit(J)
H_d	Heat delivered within the IEG(J)
Hc	Charging frequency(s^{-1})
I	Discharge current (Ampere)
Q	Rate of heat supplied at workpiece (W)
q'	Heat supplied (J)
$Q(t)$	Rate of heat flux supplied in W/mm^2
A	Area over which heat flux is acting (mm^2)
MRR_d	Material removal rate per discharge (mm^3)
MRR	Material removal rate (mm^3/min.)
γ_{cr}	Critical concentration ratio (N_{cr}/N_∞)
N_{cr}	Particle concentration at breakdown (g/l)
N_∞	Average particle concentration (g/l)
R_{pc}	Critical radius (mm)
t_B	Break down time (μs)
$K_Ø$	Constant
x	Inter-electrode gap (mm)
s	Size of individual powder particles (mm)
E	Electric field at a location other than discharge region (V/mm)
Eo	Electric field at discharge region (V/mm)
P_{on}	Pulse-on time (μs)
P_{off}	Pulse-off time (μs)
V_{vt}	Total crater volume (mm^3)
j_i	Volume of individual cylindrical discs(mm^3)
W_i	Initial mass of the workpiece before machining (g)
W_f	Final mass of the workpiece after machining (g)
ρ	Density of the workpiece (g/mm^3)

T_m	Machining time for experiments (minutes).
η	Viscosity of dielectric medium (Pas)
EDM	Electrical-discharge Machining
IEG	Inter Electrode Gap (mm)
PMEDM	Powder mixed electrical discharge machining
ND-EDM	Near dry electrical discharge machining
PMND-EDM	Powder mixed near dry electrical discharge machining

CHAPTER 1

INTRODUCTION

1.1 NEED OF ADVANCED MANUFACTURING MACHINING METHODS

Industries like automobile, aerospace, power plant (nuclear reactors), railways etc. are comparatively more technologically advanced than other industries like metal cutting, steel rolling mills and paper manufacturing industries etc. Also, in these industries there are strict guidelines from buyers and manufacturers to follow closed dimensional accuracy, pin-point precision and uninterrupted efficient functioning of components for a long run. Therefore, there is always a great demand of advanced materials (like high temperature resistant alloys having high strength for e.g. Tungsten carbide) and advanced techniques for their machining in these kind of industries. Material science researchers are always thriving towards achieving highest strength, hardness, toughness and other diverse properties through these kinds of advanced materials. Discovery and production of these kinds of advanced materials is already a very wide research area and it is actually increasing our understanding regarding the application of vivid technologies for achieving the desired properties in the material as per our needs.

It is always seen that low production rate or lower economics of machining is associated with work hardening of the workpiece. This work-hardening phenomenon is natural and it occurs as long as the material is machined continuously. And in case of materials like tungsten, titanium, high speed stainless steel, fiber-reinforced composites, stellites, ceramics, cermets and nimonics it becomes almost impossible for a machine tool to machine complex or even simple shapes on them. Other most sought after requirement regarding the applications of these advanced machining processes are manufacturing of non-circular (like elliptical holes), micro-sized, large aspect-ratio, narrow entry angled, single or a cluster of

holes within a workpiece. Contoured holes and burrless holes making in hard-to-machine materials can also be done through advanced machining techniques.

These advanced machining or non-conventional machining processes are developed in a long duration of time. These processes differ from the conventional ones in a way that they use energy in its direct form for removing the material from the workpiece. Some of the advanced machining processes that are used in industries are as:- Electrical discharge machining, Plasma arc machining, Laser beam machining, Electron beam machining, Ion beam machining, Abrasive flow machining, Ultrasonic machining.

With these processes, one can remove material from inaccessible locations within the workpiece for eg. creation of cooling vents in a turbine blade by electrical-discharge machining process which is impossible with any conventional machining process. Certain other areas where it is inevitable to use/prefer non-conventional methods over conventional ones are as :

- Brittleness of workpiece is very high like that of a glass, highly heat-treated alloys, ceramics and powder-metallurgy parts.
- If parts are too tender/soft/flexible to sustain the heavy forces of mechanical/traditional machine tools like forces produced by grinding wheels. In some cases limitations in clamping and fixturing of workpieces (like cutting of meat) also restrain user to abstain conventional methods and move over to non-conventional ones.
- If there is a possibility of rise in temperature and residual stresses at an uncontrollable level in the machined workpiece for example in grinding.

All these above difficulties actually were the reason for invention and flourishing of these kind of non-traditional machining processes which use chemical, laser, electrical, high-energy beams as sources of power for wearing material from metallic and non-metallic workpieces. With these non-traditional machining processes removal of material does not occur in the form of chips instead they come out in the order of microns. And this wear occurs through chemical dissolution/reaction, etching, evaporation, hydrodynamic actions, melting and at some instances through action of abrasive particles. The salient feature that catches the attention of every user of non-conventional process is that their efficiency does

not depends upon the nature of workpiece (like hardness) material which they are machining. These process are preferred over their traditional counterparts because of their ability to produce striking technological and economical merits. Infact, Taniguchi [4] proposed and inferred that very high accuracies and tight tolerances cannot be achieved merely by using precise conventional machining methods where removal of metal is usually in the form of chips. On the other hand these tight tolerances and higher level of accuracies can be easily obtained through non-traditional methods.

1.2 A BRIEF NOTE ON ADVANCED MACHINING PROCESSES

In AFM (Abrasive flow machining), AJM (Abrasive jet machining), USM (Ultrasonic machining) and WJM (Water jet machining) the kinetic energy of abrasive particles or the medium is used for removal of material from the workpiece. In AWJM (abrasive water jet machining) kinetic energy of abrasive particle and flowing water both are utilised at the same time. Provision of magnetic brush in magnetic abrasive flow machining helps in reducing surface irregularities from pre-machined surfaces. In AFM hydraulic pressure is applied on the abrasive slurry to provide kinetic energy to it so that it can remove unwanted material from the workpiece. Thermo-electrical methods like Plasma arc machining (PAM), Laser beam machining (LBM), Electro-beam machining (EBM) and EDM uses energy in the form of heat, light, electron bombardement and electrical arc respectively for removal of material from the workpiece. Chemical machining and electro-chemical machining utilises chemical reactions and electrically assisted chemical reactions respectively between the workpiece. Biochemical machining is in use for machining biodegradable plastics.

While selecting a machining process the following factors should be taken care of :

- Process capability
- Properties of material to be machined
- Physical parameters
- Shape to be machined
- Economics of the process.

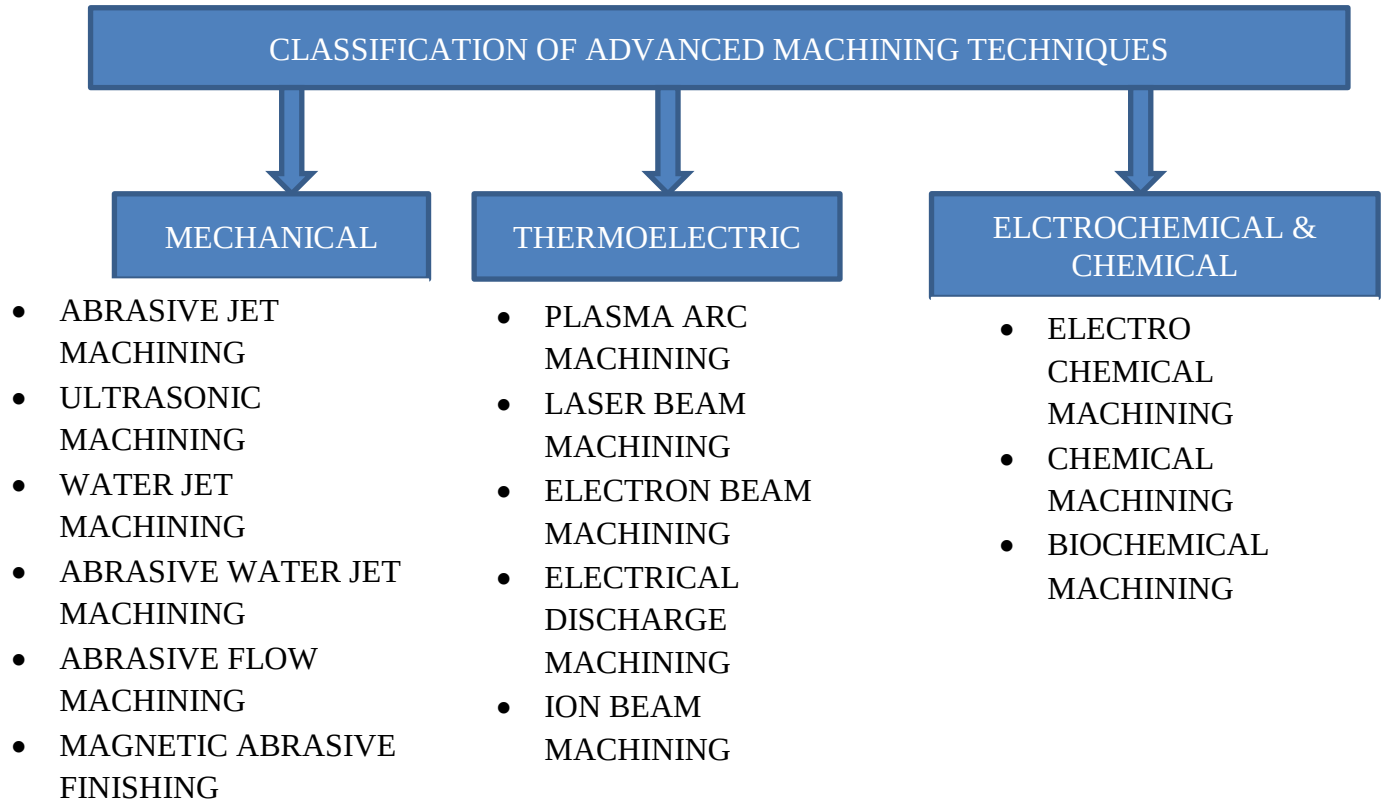

Fig 1.1 Categorisation of Advanced Machining Methods

1.3 HYBRID PROCESS

Due to a recent increase in demand of micro-level components in diverse fields like bio-medics, aerospace, power generation, optical and electronics industries a whooping increment in production of these kind of products has also increased. Although some highly accurate and advanced traditional manufacturing methods are available for production of these type of products but reaching the desired mass production level is a highly elusive prospect. On the other hand, some non-traditional techniques are also their for the same purpose but problems like accuracy, efficiency and versatility of these manufacturing processes exist. So for avoiding this problem some special processes are devised they are actually a combination of two, more than two non-conventional machining processes (NCMP) or one conventional and one non-conventional processes. These group of processes are combined as an individual process so that merits of each individual process can be used collectively and effectively. It can be easily understand by an example like a general grinding process is associated with good surface finish and lower values of tolerances but this process imparts burrs, heat affected zone and residual stresses in the workpiece. On the other hand, machining through electrochemical machining process avoids these demerits.

This lead to the development of a hybrid process called Electro-chemical grinding. Similarly, finishing of a part improves its aesthetics and functional performance i.e. the fine finished parts have better dimensional controls, endurance strength and thus longer working life. In the recent times, the requirement of finely finished products with close dimensional controls along with increasing complexity in their shape is tremendously increased. For such finishing requirements, Abrasive flow machining (AFM) process is a most suitable non-conventional finishing process. It is a non-traditional polishing process to polish metallic components using a semi-liquid paste, and with this complicated or miniaturized parts requiring high surface finish can be economically produced [2]. Extrusion of abrasives laden media (mixture of a liquid polymer with abrasive particles) through a controlled passage results in the abrasion of the desired unwanted surfaces due to the cutting action of a number of randomly oriented cutting points of abrasives. This process is mainly suitable for the complex shaped internal cavities or for the fine finishing of micro size holes/slots (even for the simultaneous polishing of different cavities).

Although there is no precise classification of hybrid machining processes but according to the extent of contribution of each individual machining process in a given hybrid machining process the hybrid machining process is classified into two categories viz. a) Assisted hybrid machining process and b) Combined hybrid machining process[3].

In assisted hybrid machining technique one machining technique, generally a non-conventional one is super-imposed on the conventional machine tool, the non-conventional technique generally comprises of a particular source of energy or a combination of various different energy sources. Certain assisted hybrid machining techniques are :- vibration-assisted milling, vibration-assisted grooving, vibration-assisted engraving, vibration-assisted grinding, vibration-assisted drilling, vibration-assisted polishing, vibration-assisted EDM, vibration-assisted ECM and vibration-assisted laser machining etc. In vibration assisted machining techniques mainly ultrasonic vibrations are used.

Combined hybrid machining process work on the concept that all the contributing micro-machining processes work together for the material removal at the same time and hence they influence the machined area simultaneously. Their

ability to mass produce parts with mirror-like surface finish, tight dimensional tolerances, improved machining rate within a very small interval of time. some common and most sought after combined hybrid machining processes used in industries are Electrochemical discharge machining process, Electrochemical discharge milling, Electrochemical grinding process, EDM-Electrorheological fluid-assisted polishing and Laser drilling-jet ECM etc.

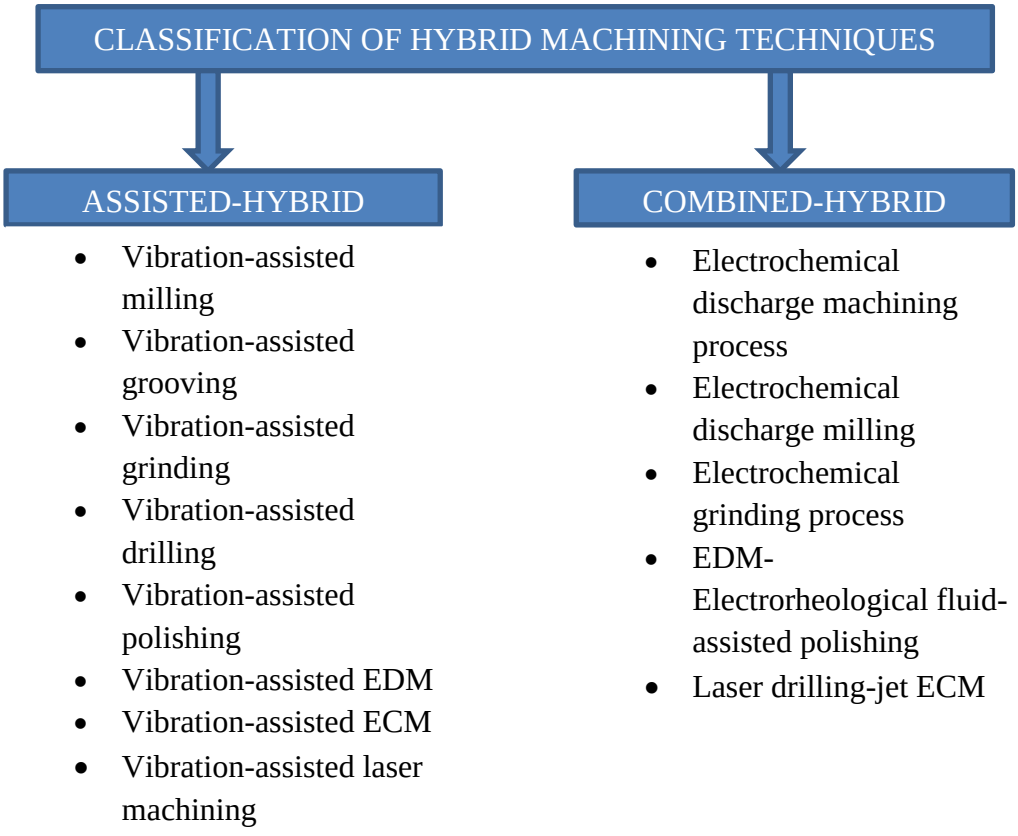

Fig 1.2 Classification of Hybrid Advanced Machining Methods

Apart from this, the hybrid machining approach paves the path of new frontiers in research work of advanced machining processes. These future research scopes regarding the development of hybrid machining processes are as follows:-

- Determining the working mechanisms of these processes
- Developing different modelling techniques which can best depict the the give hybrid machining process.
- Evolving the simple hybrid process into more versatile ones by fabrication of multi-axial extremely precise machine tools.
- Application of more precise and sensitive process monitoring and controlling techniques.

- Research regarding cost potency of the process.
- Study regarding industrial viability and applicability of the process.
- These research areas can certainly develop, enhance the productivity, effectiveness, versatility, accuracy and preciseness of these non-traditional machining processes.

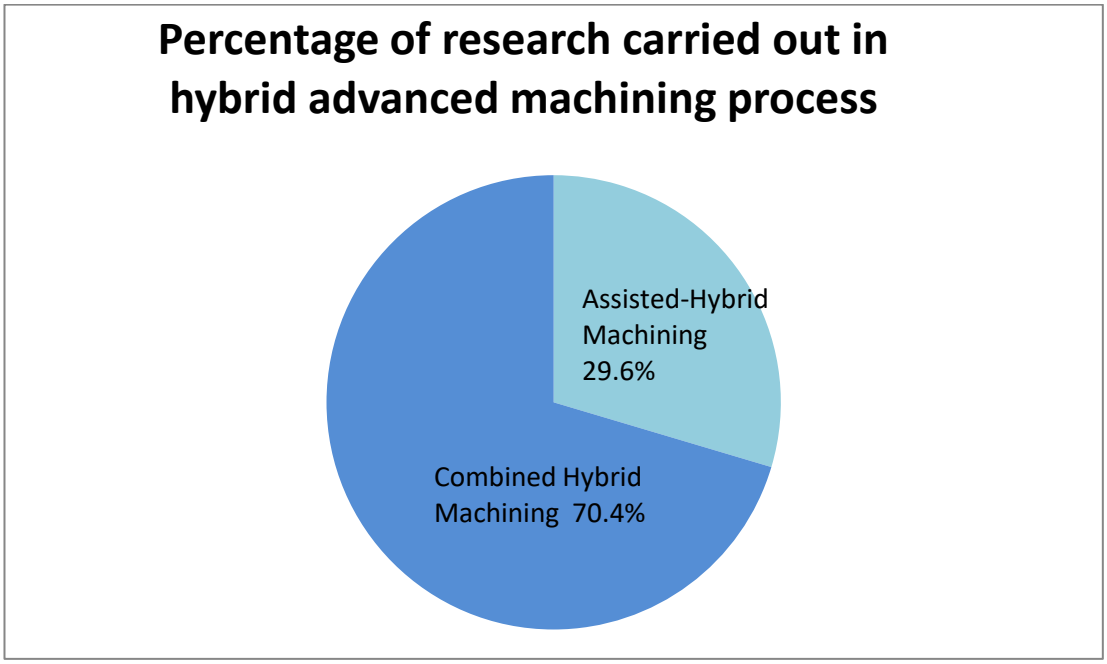

Fig. 1.3 Percentage of research performed in hybrid micro-machining processes (Peter Fonda et.al., 2007).

1.4 A BRIEF NOTE ON EDM

EDM is regarded as most familiar thermo-electric non-traditional process working on the phenomenon of electric discharges assisted material removal. This technique was invented by Russian scientists Lazarenkos and Zolotykh, [2]. The evolution of EDM process from a mere innovation in material removal technology to a highly precise practical and economic material removal process can only be attributed to the myriad number of changes and modifications introduced within in this process to cater the demand and challenges of machining advanced materials like super alloys, heat resistant steel, stainless steel and it's various types, composites and ceramics etc. over the time. These kind of materials find a whooping amount of application in die and mould-making industries, nuclear industries, railways and aerospace industries because of their high strength to weight ratio, high refractiveness, red hotness, and hardness etc qualities. The EDM technology has

evolved itself from manufacturing small components to components at micro scale over the time. Fig.4 shows the typical die-sinking applications in overall manufacturing operations.

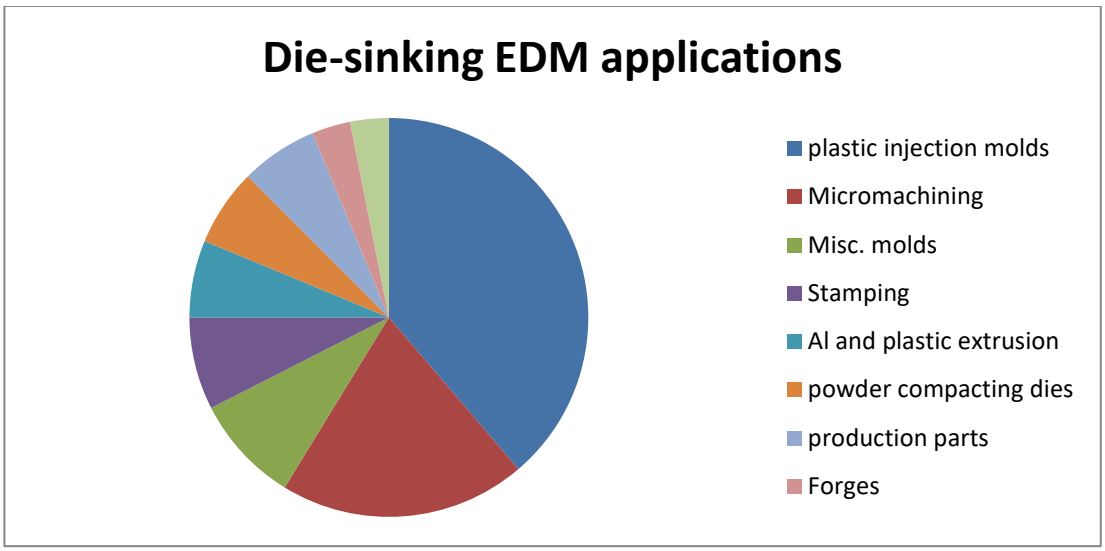

Fig. 1.4 Typical die-sinking EDM applications (Peter Fonda et.al., 2007)

Due to the absence of workpiece and tool contact material removal rate for the process is not affected by hardness, toughness and strength of the material of the electrode material must be electrically conductive. Rise in the popularity of the EDM has following reasons :

- Ease of machining intricate shapes on difficult to machine materials like glass and tungsten.
- Conformability to micro machining.
- Scope of complete automation: Current trend in EDM industry indicates that the use of automatic tool changing in addition to feed-back control systems is quite necessary and very productive. This allows an uninterrupted and efficient running of EDM machine for an overnight or for more longer periods. If artificial intelligence can be used for controlling of machine then the dream of a fully automated EDM machine tool can be achieved.
- Preciseness and accuracy of the process
- Insensitiveness towards the hardness and strength of the workpiece material.
- Negligible presence of cutting forces on workpiece during machining.

Inspite of all the above mentioned superiorities over conventional ones a severe drawback of EDM process is that the fumes of burned dielectric medium emanates during machining which are actually harmful for human health. Although

dielectric fluid plays a very important role in EDM as it is responsible for cooling of tool and workpiece, flushing of debris of machining within the inter-electrode gap and concentrating the sparking energy to a particular region of interest. Controlling of IEG also very much depends on the working of dielectric fluid which in turns is responsible for monitoring the spark energy and frequency of occurrence of sparks. That's why various attempts were made in past to limit the evolution of these kind of fumes by using some innovating techniques which can transform the EDM from a hazardous to an eco-friendly machining process.

A huge amount of research work had been done to make it possible. One such attempt was by Kuneida et al. [5] Their team were the first to suggest that EDM can be economically performed in the presence of a gas dielectric medium. After that Tao et al. [6] proposed various different dry EDM strategies.

In PMND-EDM (powder mixed near dry electrical discharge machining), a powder mixed mixture of single, dual or multiphase dielectric medium is used and this whole thing is done in the presence of a gas dielectric medium (as one of it's phase) like air. Due to reduced amount of usage of hazardous liquid medium lesser amount of harmful fumes get into the atmosphere and hence machining becomes more eco-friendly or we can say conducive to humans.

1.5 WORKING PRINCIPLE OF EDM

Being a thermoelectric process, EDM uses spark as a heat energy source for erosion of material from the workpiece and regrettably from the tool also. An essential condition for EDM to take place is that both tool and the workpiece material must be electrically conductive in nature. Tool and the workpiece are always kept at a distance in the order of 25-50 μm so as to hold the favourable conditions for production of spark, by the way a minimum gap width is maintained for initiation of spark. Although sparking (single spark) last only for few micro seconds but the frequency of sparking is in the order of ten thousands spark discharges per second. Area or location where the spark strikes is quite small mostly in the order of few sq. mm but this same area is always under a tremendous amount of thermal load (heat flux) as a result of which temperature in this region reaches upto thousands of degree celsius depending upon the dielectric strength, current and voltage supply. As a result of these high temperatures the material at the workpiece and tool tend to melt and

vaporise around this region. In this way desirable material removal take place at workpiece end with a hugely undesirable metal erosion phenomenon at tool simultaneously. Most of the times material is removed in the form of craters, the shape of these craters solely depends upon the type of EDM and the level of process parameters selected . A mirror image of tool face gets imprinted on the workpiece. This image/shape would be more identical only if the erosion of tool does not take place and this thing is ensured by choosing the process parameters and polarity of electrodes advertently.

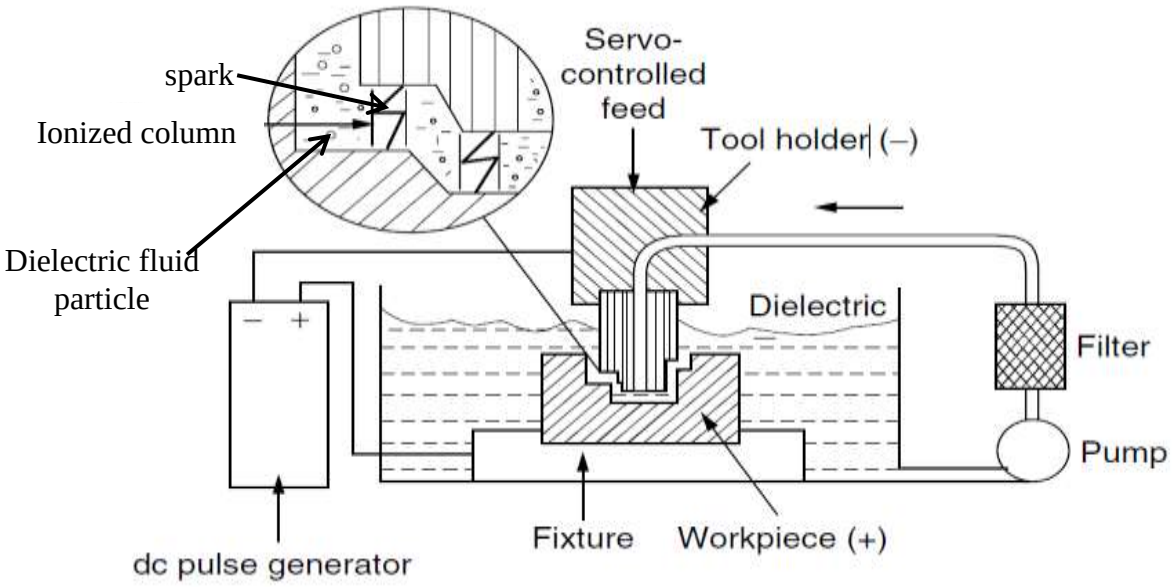

Fig 1.5 Schematic diagram of EDM system.

During the machining the material at workpiece and electrode get eroded and came in the form of minute particles. Debris is the name coined for these eroded particles from both electrodes. This debris is generally of asymmetric and random shape, as it is a by-product of unrestricted multi-directional solidification of molten eroded material. They can be of hollow spherical shapes also.

Comparatively a very less amount of material is lost from the tool. Generally, a micro level gap is maintained between tool and workpiece. This gap has to be maintained throughout the machining operation and this is ensured by utilising servo system to maintain/control the motion of tool towards the workpiece.

EDM utilises a pulse dc voltage supply in the order of 80-100V at 5kHz at the same time the irregular surface of the workpiece and tool full-fill the required condition for minimum gap across the region. Due to these two conditions an intense

electric field of magnitude 10^5-10^7 V/m is estabilised at the gap. Due to this highly intense electric field the movement of electrons (as they are detached from cathode) from cathode to anode within the dielectric material takes place. This also results in removal of electrons from the neutral molecules of dielectric medium and this enhances ionisation. A persistent and consistent conductive channel is estabilised in the presence of highly intense ionisation. Here a huge number of electrons from cathode, migrates towards anode and that of ions towards cathode (or tool). These movements give rise to kinetic energy in them, then this energy further get converted into heat energy as striking of ions results in heating of cathode and on the other hand anode is severly heated by fast moving electrons. The whole phenomenon give rise to a momentary strong stream of current/spark within the IEG(inter-electrode gap) and due to which a tremendously huge amount of localised temperature gradient is estabilised. This high temperature results in melting or even the vaporisation of material from both cathode as well as anode. Vaporisation of metal is suppressed by the very high pressure region (around 200 atm) created by evaporation of dielectric medium. But as the pulse get into off phase (i.e. when spark extinguishes) then the vaporisation of dielectric started diminishing creating a favourable environment for vaporisation of superheated metal. As metal removal solely depends upon amount of bombardment of charged particles received by the cathode and anode hence it can be controlled by only means like tweaking the values of voltage, current and providing other conditions for estabilishment of strong arc at IEG in the presence of efficient flushing conditions.

In general, straight polarity in which workpiece is kept as anode and tool is kept as cathode but in some case reverse polarity (opposite of straight polarity) but in some case applicable as shown in fig.1.6. Normally, EDM is carried out in two stages according to the use viz., high MRR rough machining with rough surface finish and low MRR fine finishing with high quality surface finish. A minor image of tool is formed on workpiece as sparking occurs all over the workpiece surface.

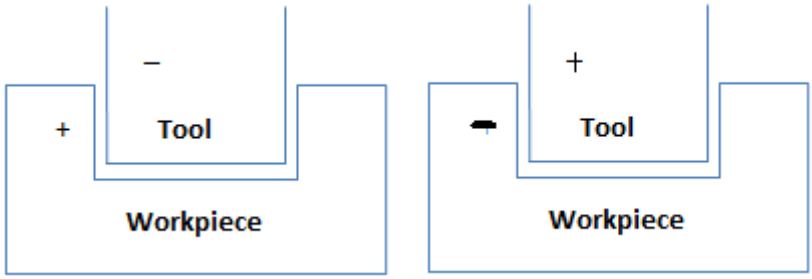

(a) (b)

Fig 1.6 Diagram depicting (a) straight polarity and (b) reverse polarity in an EDM circuit.

1.6 PULSE GENERATOR

Pulse generator is responsible for generating pulse of desired specification for particular application. Certain salient features of RC pulse generator are as

- Long idle time and a very feeble spark time results in low values of MRR.
- A reduced MRR is necessary for fine finishing.
- High wear rate for tool.

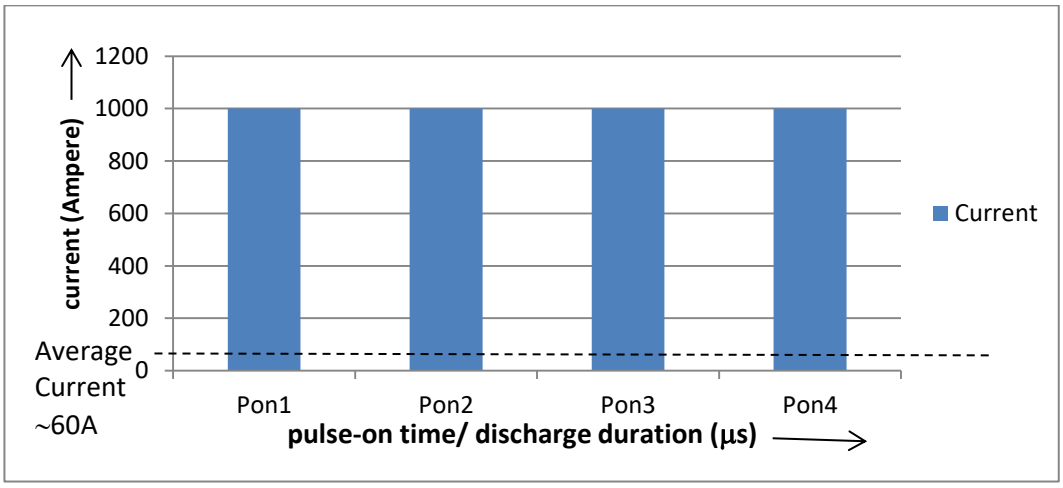

Fig 1.7 Diagram depicting relationship of peak current and pulse-on time.[1]

Form the fig. 1.7 it is clear that level of current in RC circuit is very high. This much of temperature can severely deteriorate the surfaces of both workpiece and tool. This severe temperature ranges are controlled by employing a controlled pulse generator. The peculiarity of these type of pulse generators is that they provide low value of maximum current, diminished idle time and enough pulse length which can be easily applied according to the application like for rough machining and fine machining.

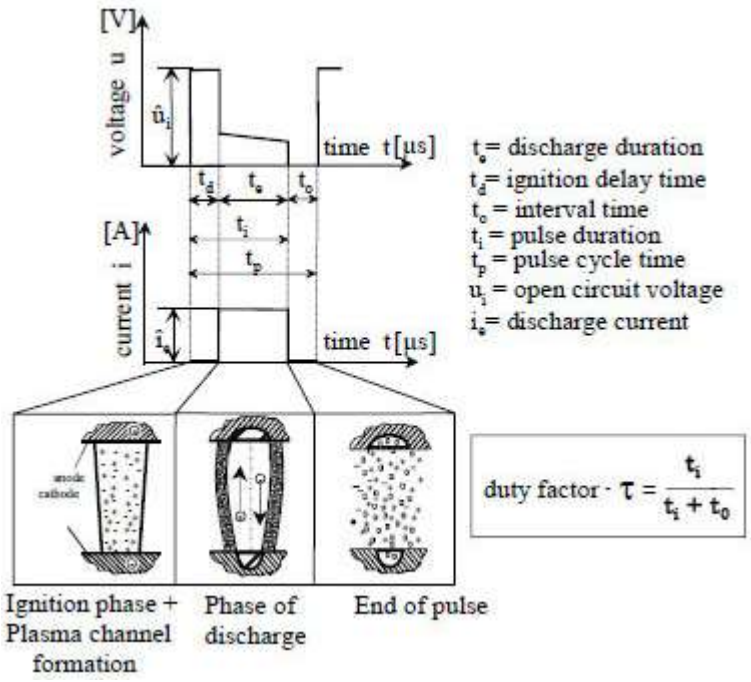

Fig 1.8 Voltage and current developed by controlled pulse generator. (Fred Lacerda et.al., 2010)

1.7 EDM MACHINE

Regarded as most promising non-conventional machining process that's why EDM is used as a medium to perform most complex and fine machining within the industries. A typical EDM machine has four important components. They are power supply, dielectric system, tool(electrode), workpiece and servo system as shown in Fig 1.9.

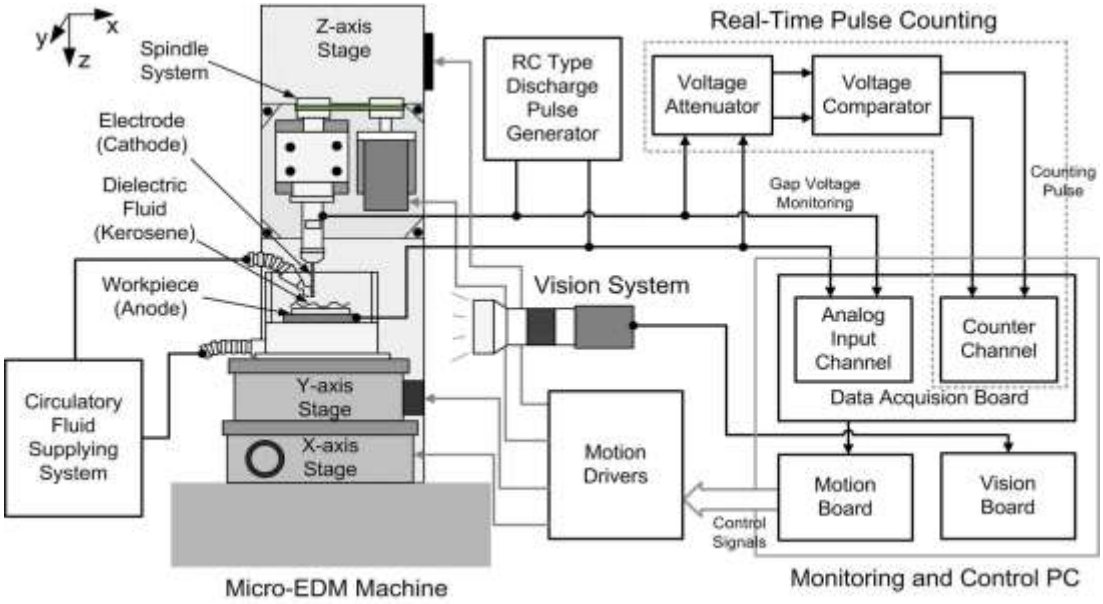

Fig 1.9 Main components of an EDM system. (Jae Won Jung et.al., 2008)

1.7.1 POWER SUPPLY

Since an EDM machine works upon DC pulses, so AC power supply is conditioned through a solid state rectifier which transforms it into DC supply. Some part of this DC supply is used to form a square wave signal which is a form of a pulse, this process is done through a multi-vibration oscillator.

A bank of power transistors acting like high speed switches are triggered by these dc signals, which further controls the flow of rest of the power. As a result high intensity pulse are obtained as output which further used in creation of sparks between the electrodes (within the IEG). It is the limitation of power system due to which it can create spark up to or within certain inter-electrode gap range at a particular voltage supply. So for a particular voltage supply the gap between electrode and workpiece is maintained by a servo system. It is the prime function of power supply system to put a check on the value of voltage, current, duty-cycle and electrode polarity.

Duty cycle is the ratio of pulse-on time and total pulse time. In this way, it gives the information about how much time the energy existed during a single pulse duration. Provision of power cut-off is always there so as to protect the circuit from electrical failures. This is done through a power cut-off protection circuit. This unit immediately act if either a spark is initiated within the IEG or when it is cut-off as a result of upsurge in voltage and current value. The possible four states that can occur while machining on EDM are as normal discharge, free discharge, short-circuit and open circuit. A pulse generator is used to detect which among these four states is taking place within the circuit. The basis of this detection and discrimination is the concept of variation of voltage with respect to the time.

1.7.2 DIELECTRIC SYSTEM

Dielectric system is responsible for efficient and uninterrupted supply of dielectric medium within the IEG so that essential machining conditions are satisfied during EDM. Delivery valves, reservoir, filters, dielectric fluids and pumps are components of a dielectric system. The salient features of a good dielectric system are as follows:-

- It should have huge magnitude of dielectric strength

- Must be efficient enough to maintain minimum ignition delay as the breakdown voltage is reached.
- Strong neutralising power to remove the charges on the charged particles from the IEG just after the extinguistion of the spark.
- Should have better cooling abilities so that it can work efficiently as a coolant.
- Low viscosity so as to provide effortless flushing of debris and worn out dielectric fluid form the system.
- Must be non-corrosive and least chemically reactive.
- Dielectric which are prevalent in industries and labs are kerosene, de-ionised water, lubricating oils, paraffin oils and transformer oils etc.

Deionised water is used for high MRR applications. It has very good cooling properties but suffers from drawbacks like high tool wear rate and corrosion causing medium. For prevention of corrosion, certain kind of inhibitors are used but they give rise to electrical conductivity up to an unprecedented level which are non-negotiable. Preferably used in Wire-EDM and drilling of small diameter holes. It is ensured that dielectric must be filtered prior to recirculation so that its insulation/dielectric strength is restored or maintained. Filtration is done for removing debris as the fine as 2μm. as the machining progresses the presence of debris materials (particles) increases within the gap and this should be cleared as new dielectric has to fill in the IEG. This problem becomes even more worse if intricate shape tools are to be used. Therefore, role of flushing becomes very decisive for productivity and preciseness of machining.

Inefficient flushing can lead to low MRR, poor surface-finish and loose dimensional tolerances. Kosy et al., [7] suggested that effective flushing can enhance the MRR by a factor of 8 to 10. Apart from that poor flushing can also leads to clogging of debris and burned dielectric within the IEG which leads to unwanted short-circuiting and arcing. It is a major responsibility of the flushing system to send the dielectric to that place where sparking needs to be done. Proper flushing of blind cavities is very difficult. Various flushing techniques that can be utilished while machining [53] are as :-

- Injection flushing
- Suction flushing

- Side flushing
- Flushing by dielectric pumping

1.7.2.1 INJECTION FLUSHING

Flushing medium or dielectric is continuously provided through a indentation or hole either in tool or in the workpiece.

1.7.2.2 SUCTION FLUSHING

Here, suction of fluid take place either via tool or through workpiece. In this case, drawback like taper effects are avoided. Suction via tool is provided to be more efficient and fruitful than via workpiece.

1.7.2.3 SIDE FLUSHING

In this method, the whole surface of the workpiece and tool is covered by the flowing dielectric fluid must be ensured.

1.7.2.4 FLUSHING THROUGH DIELECTRIC PUMPING

Pulsative movement of electrode tool is used to allow the dielectric fluid to suck into the IEG and then removal of the debris (as the tool is lowered down). This kind of approach is mainly used in deep hole drilling applications.

Flushing of blind holes is more problematic than their machining. Mostly, in this case a hollow tool is used to provide dielectric at the machining site but this provision results in bump like impression right beneath the hollow part of the tool over the workpiece. This problem is solved by using a tool with eccentric holes.

Jet flushing is an another mode of flushing used in EDM. Basically it is used where there is a limitation of using other flushing method due to some shape and size constraints of tool and workpiece.

For avoiding the fire due to inflammable dielectric, it is always preferred to sink the whole workpiece with the dielectric fluid. Due to continuous machining of workpiece debris get accumulated at the IEG, this results in bridging of the gap. Due to this more number of sparks/arcs get into the picture which results in undesirable deterioration of workpiece and tool surface. This same drawback is

utilised in PMND-EDM in which more electrically conductive powder particles (other than workpiece) are used. These powdered particles are mixed with the dielectric material or fluid. Being more electrically conductive than workpiece material they enhances the number of sparks and also they provide better conduction of uniform heat to the workpiece which results in more material removal rate with better surface finish. During EDM, continuous filtration of the dielectric material must be done simultaneously with machining so that the debris generated did not get clogged up at the IEG.

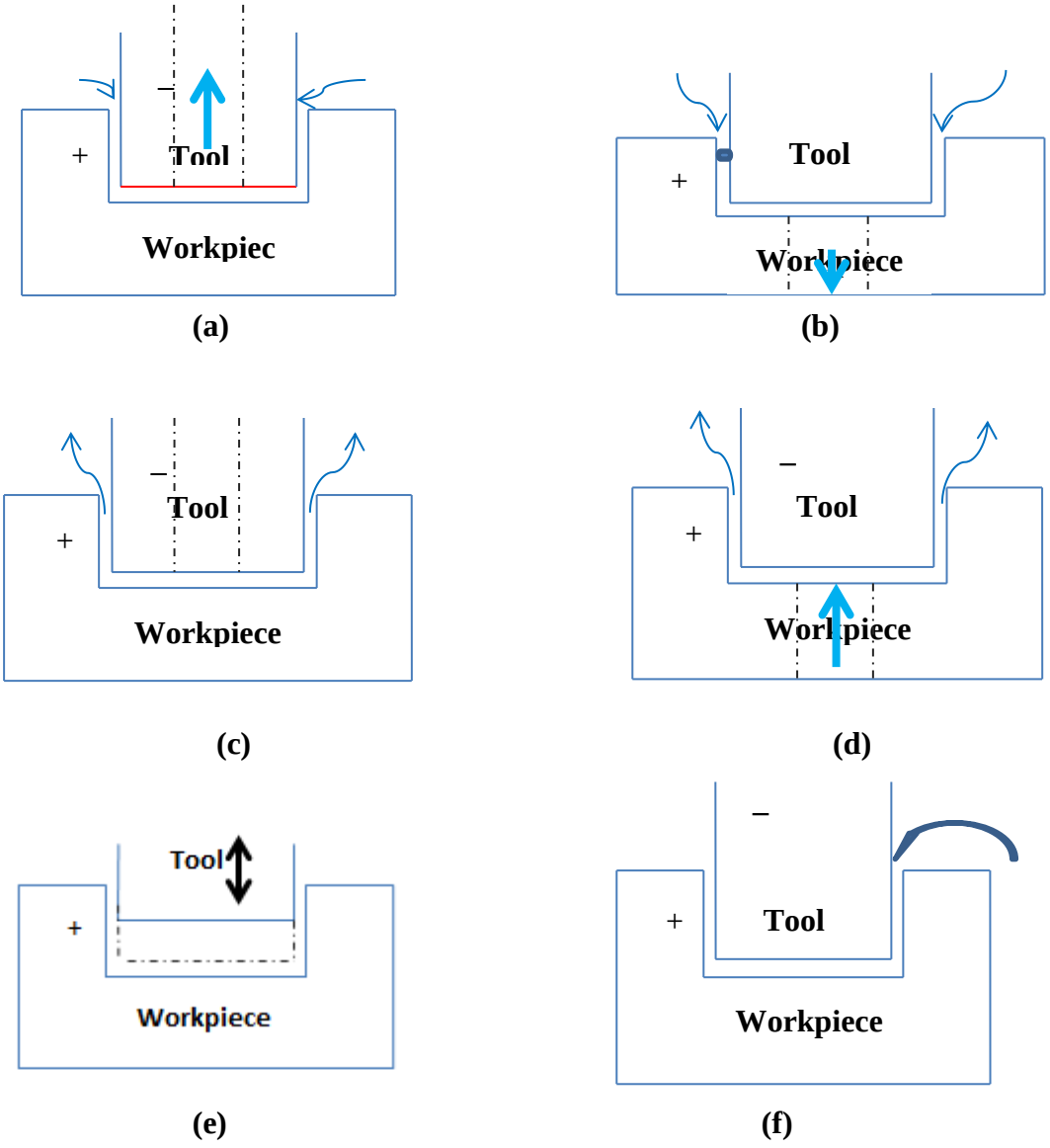

Fig 1.10 Various methods for dielectric flushing: (a) suction through electrode, (b) suction through workpiece, (c) pressure through electrode, (d) pressure through workpiece, (e) periodic cycling of electrode, (f) jet flushing [1].

1.7.3 ELECTRODES

Workpiece and tool are actually electrodes but generally tool is termed as electrode in EDM. Since they are essential part of EDM process so it is desired that they should posses certain salient features so as to facilitate efficient and effortless machining. The desirable properties which a tool electrode should have in EDM are as :-

- Good machinability
- Better electrical and thermal conductivity
- Low cast
- Abundancy
- Low reactivity and corrosiveness
- Low brittleness

Some of the materials which can be a good candidate for being a tool in EDM are as

- Copper and brass: As they have low wearability and are highly chemically stable at high temperature.
- Copper and tungsten: As it has low wear rate but comes with drawbacks like poor machinability and high cost.
- Other materials are copper, boron, cast aluminium and silver tungsten.
- Graphite: It has got high value of electrical and thermal conductivity, it is less wearable and can be easily machined. Graphite tool having fine grains wears very less, provide good surface finish to the workpiece and results in higher levels of MRR. But due to its brittle nature it is very much prone to break during machining.
- Due to inevitable electrode degeneration, it was prefered to have higher finishing allowance values as it compensates for overcut but this always lead to a increase in machining time for having a finishing cut.

A huge amount of work has been done due to encounter this electrode degradation problem. Tricks like controlling the pulse rate and its shape, considering advanced tool materials and choosing conductive machining conditions helped researchers to achieve a low wear rate of tool. That’s why it is preferred to have a tool having striking resemblance with the shape and size of workpiece so as to get very fine machining. A simple example of overcut is given in fig. 1.10 a. During electric-discharge drilling (EDD), overcut has to pre-estimated and prior machining,

better at the designing phase. Generally, the electrode/tool losses its material from its corners because the magnitude of electric field intensity is very high at this point.

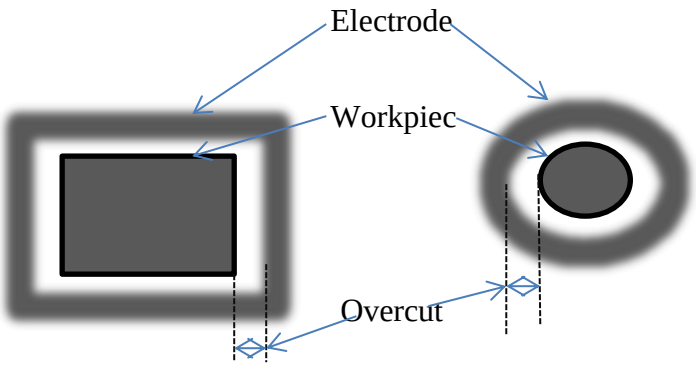

Fig 1.11 Diagram illustrating the overcut developed during Electrical discharge drilling.

Wear of the tool in EDM is expressed by a tense ‘wear ratio’. It is the ratio of metal being being worn out from the tool to the material removed from workpiece. It’s value can range from 0.05:1 to 100:1. To avoid the chances of extreme wearing certain techniques can be employed in EDM for particular type of machining for example if a through hole has to be drilled into the workpiece EDD. But in this case machining time will be very large and it may be possible that tool will wear at a tremendous rate. So for avoiding this, an operation called electric-discharge trepanning can be employed. In this case, only a small thickness present outside the periphery of desired hole is removed and hence a hole is drilled.

1.7.4 SERVO SYSTEM

The main objective of a servo system is to maintain a desired amount of gap (or inter-electrode gap) between the tool and the workpiece. For this, it employs a gap voltage sensor which works consistently to sense the gap and anything in between this gap like presence of some electrically conductive particles. After receiving the signals from the gap voltage sensor the servo system directs the tool to move up, down and flush out any kind of conductive particle if there with the use of flushing dielectric medium.

The major requirements for an efficient servo system are as:-

- It must be sensitive towards minute movements of the tool.

- It must sustain and work efficiently against the weight of electrode, ram and action of flushing forces.

1.7.4 ELECTRODE REFEEDING

The necessity of tool refeeding arises due to the fact that with every successive turn of machining the tool looses its shape as well as its length. And if this shortening of length is not compensated regularly then it will definitely effect the extent of machining like in drilling the length of hole produced will be smaller than desired length. One way to overcome this problem is by introducing exactly that much amount of new electrode that has been worned out. Other way is to brought back the electrode at a particular reference sight/point every time the drilling of hole is done and from there the extent of drilling done is estimated. Refeeding of electrode is done either normally or automatically.

1.7.5 CNC-EDM

Introduction of CNC technology within an EDM machine tool has made it more effective, productive, user-friendly, protean and efficient. Through this technology it becomes easier for manufacturing firm to carry out uninterrupted machining operation for an overnight or for many days in continuation. Complex machining like machining of helical gears becomes very easy due to provision and use of canned cycles. Fine finishing can be achieved easily through CNC-EDM as it involves almost nil amount of involvement of humans. Same worker who previously use to look after the machine now has ample amount of time to think over other aspects of machining of machining can utilise this time for making strategies for other jobs.

This mode of working of CNC-EDM is governed by its adaptive control(AC). In this all the power supply parameters and electrical signal sampling against pulse interval for each individual pulse is carried out so that any unwanted arcing can be eliminated. An interesting advantage of using CNC system is that orbiting of electrode becomes versatile (as nowadays it is governed by softness rather mechanically) and due to this improved flushing efficiency is obtained.

Due to this AC system, periodic retraction of the tool can be obtained in a very easy way which again is very helpful in increasing the efficiency of the

machining process. Thus through AC, maintaining and controlling of spark energy can be easily handled which allows to achieve “no-wear condition” by the machine.

Invention of automatic tool changer (ATC) technique proves very helpful to an EDM set up. As the job of ATC is to provide different types of tools required for different kinds of tools required for different kinds of applications in a very short period of time with pin-point precision. In addition to that it also allows the automatic changing of tools within any program code. This increases productivity and maximum utilisation of machine.

So this provision of CNC technology can be applied on an EDM set up to provide different tools for various operations like rough machining, fine machining an ultra fine machining, CNC-EDM can be used attended for log periods of time without wondering about the tool change sequence.

An advanced feature like electrode zeroing is used on CNC-EDM to estimate the exact positioning of starting point for machining and this is automatically. By use of this method wear of tool is easily compensated as the depth to be machined can be controlled precisely and accurately here.

1.8 ANALYSIS

Analysing a RC-circuit is very essential for determination of amount of power getting delivered to the workpiece from the main supply, amount of charging and discharging voltage and current value attained by the whole circuit and maximum power conditions etc.

1.8.1 GENERATING EXPRESSIONS FOR VOLATAGE AND CURRENT DEVELOPED DURING CHARGING

In a relaxation-type circuit or in an RC circuit there are two main parts viz. charging unit and discharging unit. The expression of charging current (ι_c) is given as $\iota_c = \frac{V_o - V_c}{\Re_c}$ (1.1)

$$\iota_c = \varsigma_c \frac{dV_c}{dt} \quad (1.2)$$

as V_o is voltage from supply side, V_c is the voltage reached inside the capacitor at the time interval ‘t’.

(1.3)

$$\frac{dV_c}{V_o - V_c} = \frac{1}{\Re_c} dt$$

taking integration on both sides of above eq^n

$$\ln\left(V_o - V_c\right) = -\frac{t}{\Re_c \varsigma} + J_1 \tag{1.4}$$

J_i is the integration constant. Using boundary condition V_c= 0 @ t=0 to calculate J_i. This results

$$J_i = \ln V_o \tag{1.5}$$

putting J_i in eq^n 1.8.4 and solving it to obtain

$$V_c = V_o(1 - e^{-t/\Re_c \varsigma}) \tag{1.6}$$

The time interval within which the capacitor reaches 0.638 times of its charging voltage is known as 'time constant' ($\Im = \Re_c \varsigma$).

Putting the value V_c from eq^n 1.6 in eq^n 1.2

$$\iota_c = \frac{V_o}{\Re_c}(e^{-t/\Re_c \varsigma}) \tag{1.7}$$

1.8.2 CALCULATION OF POWER RECEIVED BY THE DISCHARGING CIRCUIT OF RC CIRCUIT

The amount of energy received by the discharging circuit at time 't' is

$$d\xi_c = \iota_c V_c dt \tag{1.8}$$

putting the value of V_c and ι_c from eq^n 1.8.6 respectively above, we will get

$$d\xi_c = \frac{V_o}{\Re_c}\left(e^{-\frac{t}{\Re_c \varsigma}}\right) p_o \left\{1 - \left(e^{-\frac{t}{\Re_c \varsigma}}\right)\right\} dt \tag{1.9}$$

Doing integrating on both sides

$$\xi_c = \frac{V_o^{\,2}}{\Re_c}\left(-\Im^{-\frac{t}{\Re_c \varsigma}} + \frac{\Im}{2} e^{-\frac{2t}{\Im}}\right) + J_2 \tag{1.10}$$

where $\Im = \Re_c \varsigma$. J_2 is a constant value, it was calculated by using boundary conditions like ξ_c=0 @ t=0. By putting J_2 in eq^n 1.8.10, we will have

$$\xi_c = \frac{V_o^{\,2}\Im}{\Re_c}\left(\frac{1}{2} - e^{-\frac{t}{\Im}} + \frac{\Im}{2} e^{-\frac{2t}{\Im}}\right)$$

considering that energy ξc is transferred to discharging circuit for time ℑ(= t) then the mean power transferred (H_{mean}) is depicted as

$$H_{mean} = \frac{V_o^{\,2}\Im}{\Re_c \Im_c}\left(\frac{1}{2} - e^{\frac{\Im_c}{\Im}} + \frac{1}{2}e^{-\frac{2\Im_c}{\Im}}\right) \tag{1.11}$$

for power to be maximum

$$\frac{dH_{mean}}{d\left(\frac{\Im_c}{\Im}\right)} = 0 \tag{1.12}$$

the solution of above eq^n will be $\Im_c/\Im c=0.72$. by putting this value in eq^n 1.8.6, we will get

$$V_c = V_o(1-e^{-1.26}) = 0.72v_o \tag{1.13}$$

thus maximum power will be delivered when discharging voltage reaches 0.72 times of supply voltage value. The relationship required between break down and supply voltage in order to have maximum delivery of power is given below

$$V_B = 0.72V_o \tag{1.14}$$

1.8.3 EXPRESSION FOR CURRENT IN DISCHARGING CIRCUITS

Suppose $\Re_s$, is the sparking resistance (since other types of resistances having negligible values so they are neglected). Then the current ι_d at any time 't' is shown as

$$\iota_d = -\frac{d\mathbb{Q}}{dt} = -C\frac{dV_c}{dt} \tag{1.15}$$

Also, $\iota_d = \frac{V_c}{\Re_s}$ (1.16)

So,

$$\frac{V_c}{\Re_s} = -C\frac{dV_c}{dt} \text{ or,} \tag{1.17}$$

$$-\frac{dt}{\Re_s C} = \frac{dV_c}{V_c} \tag{1.18}$$

Upon integrating the equation,

$$\ln\left(V_c\right) = -\frac{t}{\Re_c \varsigma} + J_3, \tag{1.19}$$

constant J_3 is calculated by the application of boundary condition like, $V_c = V_{co}$ @ t=0.

$J_3 = \ln V_{co}$ so,

$$V_c = V_{co} e^{-\frac{t}{\Re_s \varsigma}} \tag{1.20}$$

therefore,

$$\iota_d = \frac{V_c}{\Re_s} = \frac{V_{co}}{\Re_s} e^{-\frac{t}{\Re_s \varsigma}} \tag{1.21}$$

Energy emanated within inter-electrode gap is shown as

$$H_d = \frac{\varsigma V_B^{\,2}}{2} \tag{1.22}$$

1.8.4 EXPRESSION FOR MRR IN RC CIRCUIT

It is obvious that as the spark energy transferred into the workpiece is increased by any means like using higher values of process parameters, a corresponding increment in MRR value is observed.

$$\text{Since, } t = \Re_c \varsigma \ln\left(\frac{1}{1-\frac{V_c}{V_o}}\right) \tag{1.23}$$

And charging frequency (h_c) is shown as

$$h_c = \frac{1}{t} = \frac{1}{\Re_c \varsigma}\left(\frac{1}{\ln\left(\frac{1}{1-\frac{V_c}{V_o}}\right)}\right) \tag{1.24}$$

and MRR is directly related with total energy received at the workpiece per second

So, $MRR \propto \frac{\varsigma V_B^{\,2} h_c}{2}$ (1.25)

putting, p_B and h_c, and let J_4 be a constant of proportionality. Then,

$$MRR = J_4 \varsigma V_B^{\,2} \frac{1}{\Re_c \varsigma} \left(\frac{1}{\ln\left(\frac{1}{1-\frac{V_c}{V_o}} \right)} \right)$$

Hence, MRR $\propto 1/\Re_c$, i.e $\Re_c$ has to be brought down if we have to increase the MRR, although a very low $\Re_c$ will cause arcing. This lowest value value of $\Re_c$ at which arcing occurs is called critical resistance.

1.9 PROCESS VARIABLES

Process parameters are those physical parameters which directly or indirectly monitors the machining of a machine tools. Similarly an EDM set-up also have process parameters like current, voltage and pulse duration. Other parameters come into the picture depending upon the kind of hybridisation or upgradation brought into the given machine tool.

The effect of variation of these process variables can be observed on the values of MRR, surface finish and wear of the tool. Some of these are discussed here in brief:-

- Increasing current always brought an increase in MRR and this further results in poor surface finish of the machined workpiece.
- An increment in MRR is also experienced when the value of break down voltage increases.
- Introducing a surge in the value of spark frequency results striking improvement in surface finish. This can be understood by the fact that due to increase in number of sparks for the same pulse duration, the distribution of thermal energy becomes more uniform. This further results in decrease in crater depth but with fine level of surface finish.

- A diminishing trend in the value of IEG results in decrement of MRR as net heat received by the workpiece get reduced. But one advantage of this thing is that surface with tighter dimensional tolerances are obtained.
- An increase in pulse duration has brought reduction in material removal rate, always. As heat energy induced in the workpiece gets reduced also and this further results in reduced or poor surface finish.

There are two ways through which an EDM set get its pulsed power from, they are:-

a. Through relaxation or RC ciruitry,
b. Via high powered transistor circuitry.

In RC circuit, the pulsed power is directly related to the IEG behaviour during charging period. It is desired to use a dielectric material with high dielectric potential as this ensures that when it breaks down the energy liberated per spark should be very high.

1.10 DIELECTRIC POLLUTION AND ITS EFFECTS

Contamination or pollution of dielectric fluid can be a result of:-

a. Tool decomposition
b. Erosion of workpiece
c. Putrefaction of dielectric fluid itself

This type of dielectric contamination can interface with breakdown timing, time delay, nature of machine surface like pattern obtained on a machined surface, short circuiting, rate material removal and the gap essential for sparking. In fact concept of contamination is utilised in the powder mixed EDM to use foreign metallic particles (having more electrical conductivity than the workpiece) for getting improved value of MRR. The reason behind this behaviour is explained as, when these metallic impurities gather around the workpiece surface due to action of strong electrical field intensity near them, then this results in shorter time lag. However, these type of defects are not observed in the case of copper being used as a tool.

Presence of metallic impurities in the dielectric actually helps in increasing the MRR of a machining process. This can be understand by this fact that the metallic impurities helps in reducing the time lag for spark generation and providing the rest of pulse-time for more erosion of the material. These impurities also effect the erosion of tool electrode.

1.11 PROCESS CHARACTERSTICS

It is a well known the fact that being an advanced manufacturing technique the mechanical properties like machinability, hardness and toughness etc of workpiece cannot bother its machining through EDM. Similarly, other properties like physical and metallurgical ones cannot interface with its machining. Of many operations that an EDM machine can perform some of the most common operations are drilling, slotting, multiple hole drilling etc. through EDM we can achieve a great deal of repeatability and high level of accuracy in the range of 0.025-0.127 mm. Tight tolerances about 2.5mm. Through EDM finely machined tapered cavities ranging from 0.005-0.050 mm/cm can be obtained. During drilling a high aspect ratio of about 100:1 can be achieved but for precise drilling of deep holes use separate electrode tool for roughing and flushing technique has to be ensured.

An EDMed product basically contains three type of layers on its surface. These are recast layers, heat-affected zone (HAZ), transformed or converted layer. Recast layer are formed when the eroded molten metal is allowed to solidify on the surface of the workpiece. Because of this a solid metallic layer formed on the surface beside the crater or cavity. This happens mainly because of an inefficient flushing system which allows the dielectric fluid to solidify the molten metal before it is flushed out of the system.

Recast layer is very hard and brittle having hardness of 65HRC generally. These layers are porous and generally contain micro-cracks. It is always prescribed to get rid of this kinds of unwanted metallic layers as they degrade the surface finish of the workpiece and lowers the dimensional accuracies of the workpiece.

HAZ is situated right next to the recast layer. They are generally of 25μm thick. They arise due to phenomenon of rapid heating-cooling and also due to the presence of thermal residual stresses, cracks at the grain boundaries and as a result weakened grain boundaries are some of its characterstic features. Inside the conversion zone, departure from the original grain structure to a newer grain structure is observed.

Surface finish obtained during an EDM process is mainly dependent upon the machining conditions under which machining is carried out. Frequency of pulse and energy drawn at each spark are the two main criterias upon which surface finish of a particular EDM operations depend. As we can see increasing the frequency of pulse decreases the amount of energy at each spark available and it ultimately produce a uniform amount of heat available for erosion which results in removal of fine particles from the workpiece and thus higher order of surface finish values are obtained. Similarly, a high and an uncontrolled amount of heat liberation and sparking will result in deeper craters with poor surface finish.

1.12 GAP CLEANING

Gap cleaning is actually a process used for relieving the IEG from any kind of metallic impurities and debris through the flowing dielectric medium. It is seen that at the end of the spark, temperature at the spark zone decrease rapidly which results in cooling, due to this collapsing of vapour bubbles (of workpiece and dielectric material), the plasma channel and the arc takes place. This process is followed by abrupt flow of the the cold dielectric within the IEG. This results in sudden and tremendous eviction of molten material from both workpiece and tool. Here, forced flushing results in huge amount of material removal.

The appearance of machined surface obtained by EDM is usually of matte type. This is because in EDM, material removal in the form of small globules of workpiece material is obtained. Due to this a spherically shape crater forms on the work surface workpiece and the tool. Random, non-directional and unsymmetrical arcs are the prime reason for production of un-even rough surfaces in EDM. The size of these craters is in the range of 12.5-15μm generally and they are having a depth of 0.1-0.2μm. It is founded and proved that an EDMed workpiece generally have a low value of endurance limit in comparison to a specimen which machined on a lathe for same specifications. This decrement in endurance limit is of about 15% of the original value. It is also seen that as the pulse duration is increased this endurance limit continuously decreased. For removing these defects “shot-peening ” of workpiece is recommended after machining.

1.13 APPLICATIONS OF EDM

EDM can be used to machine any kind of material irrespective of it's hardness, toughness and brittleness properties only with a necessary condition that the workpiece material must be electrically conductive in nature .Dies that are used in wire-drawing, extrusion, forging and injection moulding are developed by this method. The material of these dies is hardened tool steels and it's various types. Manufacturing of through holes of miniature configurations can be easily achieved through this process. Application of EDM in die and mould engineering is exemplary. It is used in making components for plastic injection moulding m/c. EDM can be used for making dies for stamping, coining, forming, etc. It is employed for drilling tiny holes, orifices of complex geometries within a turbine blade. EDM is extensively used for manufacturing of small holes in fuel-injection nozzles. EDM'd dies are free of burrs and have higher life as compared to the dies made by using conventional methods. It permits the use of more durable die materials, viz carbide, hardened steel, exotic, etc. Matte finish obtained during EDM minimizes polishing time required. One of the common applications of EDM is the removal of broken taps, drills, studs, reamers, pins, etc. By using EDM, one can eliminate handwork (sharp details); we can do EDM (including rework) after heat treatment and can choose better die material without worrying about its machining problems. It can be used to produce shapes which are extremely difficult to make otherwise, viz. squares, 'D' holes, splines, narrow slots and grooves, blended features, etc.

Unlike conventional machining, no mechanical force act in EDM; hence the process can be employed to machine thin and fragile components without any danger of a damage due to such forces.

CHAPTER 2

LITERATURE REVIEW

2.1 INTRODUCTION

The research contributions available around 42 articles are reviewed on the PMND-EDM and it's thermo-physical modelling. Though lot of work has been done there is a necessity for development and estabilishment of a concrete thermo-physical model for PMND-EDM process. Therefore the present work is taken-up.

2.2 LITERATURE REVIEW

Yeo S.H., et al, [10] used several modelling approaches to characterize the electrical discharge machining (EDM) process based on electro-thermal concepts. However, each model has varied characteristics and approximation results. Important elucidation regarding the dissimilarities of each model and their similarities to the real material removal process is thoroughly studied. In this paper, five EDM models from Snoeys, Van Dijck, Beck, Jilani, and DiBitonto are analyzed in terms of the temperature distribution, crater geometry and material removal at the cathode. Comparative analyses on the material removal rate (MRR) ratio of the predicted result to experimental data for discharge energy range from 0.33 to 952 mJ showed that DiBitonto's model yielded the closest proximity of 1.2–46.1 MRR ratio. This is followed by Jilani (2 – 45.9 MRR ratio), Snoeys (3.9 – 203.2 MRR ratio), Beck (4.9 –197.7 MRR ratio), and Van Dijck (26.8 – 1399 MRR ratio). This paper also shows that the disk heat source models can be enhanced by improving the approximation of the heat flux and energy fraction.

Snoeys, R., et al, [11] used a disk heat source for simulating the heat input into the workpiece surface. The workpiece surface is assumed to be insulated at the outer area. Assumptions like presence of heat only during pulse-on time and only a fraction of total heat available at the tool is conducted to the workpiece (50%) are

made. Bessel's function is used to depict clear relationship of temperature with factors like thermal diffusivity, radius of spark and depth up to which the erosion is supposed to have taken place.

Van Dijck, F.S., Dutre, W.L., [6] developed a heat conduction model for the evaluating the total amount of eroded metal in EDM. The model conceptualised the two dimensional behaviour of heat source and use this for solving two different scenarios, which are finite and infinite dimension in the *z* direction. The analyses are only performed for the case of a finite dimension in the *z* direction, which is the simplified version of the infinite case. Assumptions like insulation of tool and workpiece over their entire surface has been proposed. One more assumption which is included says that only 50% of the total heat energy developed at the tool is conducted within the workpiece material.

Beck, J.V.,[52]. developed the mathematical model for estimating the transient temperatures in a semi-infinite cylinder heated by a disk heat source. In this model, the material surface was heated over a disk shaped region centred at the end of the heat flux. The surface was insulated except over the circular region where the heat flux strikes the material surfaces. However, since the model was not developed specifically for the EDM process, the heat flux did not take into account the fraction of energy transferred to the cathode. Results are given by infinite series, tables, figures and approximate relations. Care has been taken to provide methods for efficient evaluation of the infinite series because direct evaluation can require thousands of terms. Alternative exact methods are provided that require as few as three terms. The solution is intrinsically important but it is also a basic building block for spatially and time varying heat fluxes for finite as well as semi-infinite cylinders.

Jilani, S.T., Pandey, P.C.,[14] analysed the surface erosion in electrical discharge machining. They presented computation of single spark metal removal during electrical discharge machining operation. Relationship between plasma channel growth and material was observed and well estabilished through extensive theoretical and experimental work. A further detailed work on finding the effect of non-rectangular current pulse form on electrode wear and workpiece material removal has been done so that tool wear can be minimised.

Dibitonto, D.D.,et al, [15]developed a simplified cathode erosion model for electrical discharge machining process. This model is different from the other conduction models as it uses power instead of temperature as the boundary condition at IEG. This is a point heat source model. It is assumed that only a fraction but constant value of total heat at tool is delivered to the cathode over different values of current. A universal, dimensionless model is then presented which identifies the key parameters of optimum pulse time factor *(g)* and erodibility *(j)* in terms of the thermo-physical properties of the cathode material. Compton's original energy balance for gas discharges is amended for EDM conditions. Here it is believed that the high density of the liquid dielectric causes plasmas of higher energy intensity and pressure than those for gas discharges. These differences of macroscopic dielectric properties affect the microscopic mechanisms for energy transfer at the cathode. In the very short time frames of EDM, our amended model uses the photoelectric effect rather than positive-ion bombardment as the dominant source of energy supplied to the cathode surface.

Singh, H., [2] has done experimental studies regarding distribution of energy during edm. Here, a huge amount of experimental has been done for studying amount of heat energy conducted into the workpiece at different values of process parameters. This work focusses upon the assessment of optimum values for process parameters for improving the effectiveness and efficiencies of this process.

Joshi, S.N., Pandey S.S., [9]They had done thermo-physical modelling of die-sinking EDM process using finite element method (FEM). Consideration of a two-dimensional axi-symmetric continuum model is done for analysing the single spark erosion mechanism, numerically. Efforts like assuming Gausssian heat flux distribution, spark radius equation considering the effect of current and pulse duration, latent heat of fusion, etc., are done to picturise the machining process more realistically. This is further used for calculating the amount of erosion that has been taken place at workpiece and predicting the configuration of craters. Application of this model is further used for carrying out the research work regarding the effects of varying process parameters on the value of MRR and machining performance. Experimental studies were carried out to study the MRR and crater shapes produced during actual machining.

Shahri, H.R.F, et al., [16] Here, a huge array of previous works regarding thermo-physical modelling of EDM process is extensively studied. It ranges from analytical approaches and numerical methods to experimental techniques. Important aspects like restraints, merits, salient features, considerations and assumptions are of various models are also discussed here. Numerical modelling is done via two methods and they are FEM and FDM. Use of thermocouple and optical emission spectroscopy techniques are used for determination of temperature of the workpiece and electrode.

Weingärtner, E., et al., [17] In this paper, modelling and simulation of electrical discharge machining is done. In this work, prediction of amount of material removal with respect to time is done by using the simulation results. Better correlation between the experimental and analytical model for MRR values is observed as the latent heat of melting and other thermo-physical properties are considered in the model.

Bai, X., et al., [18] They did Research on material removal rate of powder mixed near dry electrical discharge machining. In this paper, In order to find the relationship between processing parameters and processing effect and improve processing efficiency, the MRR of PMND-EDM is studied systematically. The main processing parameters, such as peak current, pulse on time, pulse off time, powder concentration, flow rate, air pressure, and tool rotational speed, on MRR of PMND-EDM are studied in experiments. The experimental results showed that the MRR of PMND-EDM increased with the increase of peak current, pulse on time, flow rate, and air pressure, decreased with the increase of pulse off time and tool rotational speed, and increased firstly and then decreased with the increase of powder concentration. The significant test for process parameters on MRR of PMND-EDM is carried out through orthogonal design experiment. Analysis of variance for the result of orthogonal experiment indicates that peak current is significant at 99 % confidence level, pulse on time is significant at 95%confidence level, and flowrate is significant at 90 % confidence level. Full factor experiments of peak current, pulse on time, and flow rate are conducted. The empirical formula of MRR is established based on experimental results. Its validity is demonstrated.

Kuriachen, B., et al., [19] In this paper, an attempt has been made to model the spark radius of single pulse resistance-capacitance discharge experimentally. Full

factorial experiments at three different levels have been used to conduct the experiments. Capacitance and voltage were identified as the important parameter for RC discharge circuit. Spark radius was selected as the dependant variable and investigated the effect of individual and interaction effect of capacitance and voltage. In addition, based on regression analysis of experimental data, a mathematical model was developed. Finally, the prediction accuracy of the developed model is compared with validation experiments and found that it model can predict the spark radius with accuracy not less than 94%.

Sarikavak, Y., et al.,[20] In this study, single discharge thermo-electrical model of workpiece material removal in electrical discharge machining (EDM) was developed. Developed model includes generation of energy in liquid media, variation of plasma channel radius and transfer of heat from the channel by the electrical discharge. Effect of generated energy in plasma channel on workpiece removal was theoretically investigated by using different experimental parameters used in literature. The developed model finds the temperature distribution in the workpiece material using finite element solver ANSYS Workbench (v.11) software. It's assumed that the workpiece material reaches the melting point of workpiece material was removed from the surface. Electrical discharge process was simulated by using transient thermal analysis. The developed model has also been validated by comparing the theoretically obtained material removal values with the experimental ones.

Liu, J.F., et al., [32] In this study, an innovative modelling approach to account for massive random discharges has been developed based on the stochastic EDM process and probability theory. Die sinking EDM of NiTi alloys was simulated to investigate the thermal damage mechanism with the progression of massive random discharges. The temperature history profiles of both top surface and subsurface showed pulsing characteristics with the progression of massive random discharges, which resulted from high-frequency random discharging phenomenon. A large temperature gradient was also found on the area below the top surface, while it gradually decreased in the deep subsurface. The predicted "coral reef" surface topography and uniform temperature distribution across the surface showed that the proposed model accounting for random discharge phenomenon proved to be an effective approach to investigate the effect of EDM processes.

Wang, T, et al., [22]. This paper studies the single pulse discharge mechanism in gas with finite element method. In order to obtain the crater morphology with edge raised, the fluid field was simulated by ANAYS on the basis of thermal analysis of a single pulse generated by the instantaneous discharge in gas.

Zhao,Y., et al., [23]. In this study, electrical discharge machining (EDM), a non-contact thermal machining process, is proposed for machining single crystal silicon carbide (SiC) which exhibits extreme mechanical hardness. However, as a semiconductor, SiC demonstrates significantly different EDM characteristices compared with those of metallic materials. This research clarifies the EDM characteristics of SiC from thermal, mechanical and chemical aspects through experimental and analytical approaches. The heat transfer analysis of a single discharge of SiC taking into account Joule heating effect revealed that Joule heating effect can increase the surface temperature of SiC near the discharge spot considerably. On the other hand, experimental investigations on the EDM of SiC found that brittle fractures along crystal orientations occur in the EDM of SiC due to thermal shock. However, the influence of the crystal anisotropy of SiC on the EDM characteristics was not significant. Finally, the EDM mechanism of SiC was investigated from chemical aspects. Oxidation reaction was confirmed in the EDM of SiC in deionized water. All of these factors helped improve the machining rate of SiC to a certain extent.

Hoecheng, H. et al., [24]. This paper presents the correlation between the major machining parameters, electrical current and on-time, and the crater size produced by a single spark for the representative material SiC/AI. The experimental results not only show the predicted proportionality based on heat conduction model, but are also compared with common steels regarding the material removal rate. Though the crater size of SiC/Al is larger than steel, the SiC particles can interfere the discharges. For effective EDM, large electrical current and short on-time are recommended. Based on the obtained knowledge, one can proceed to the study of machinability of MMC by EDM for optimal production cycle.

Shabgard, M. et al., [25]. In this paper, an axisymmetric three-dimensional model for temperature distribution in the electrical discharge machining process has been developed using the finite element method to estimate the surface integrity characteristics of AISI H13 tool steel as workpiece. White layer thickness, depth of

heat affected zone, and arithmetical mean roughness consisting of the studied surface integrity features on which the effect of process parameters, including pulse on-time and pulse current were investigated. Additionally, the experiments were carried out under the designed full factorial procedure to validate the numerical results. Both numerical and experimental results show that increasing the pulse on-time leads to a higher white layer thickness, depth of heat affected zone, and the surface roughness. On the other hand, an increase in the pulse current results in a slight decrease of the white layer thickness and depth of heat affected zone, but a coarser surface roughness. Generally, there is a good agreement between the experimental and the numerical results.

Kalajahi, M.H. et al .,[26]. In this study, thermal modelling and finite element simulation of electrical discharge machining (EDM) has been done, taking into account several important aspects such as temperature-dependent material properties, shape and size of the heated zone (Gaussian heat distribution), energy distribution factor, plasma flushing efficiency, and phase change to predict thermal behavior and material removal mechanism in EDM process. Temperature distribution on the cathode has been calculated using ANSYS finite element code, and the effect of EDM parameters on heat distribution along the radius and depth of the workpiece has been obtained. Temperature profiles have been used to calculate theoretical material removal rate (MRR) from the cathode. Theoretically calculated MRRs are compared with the experimental results, making it possible to precisely determine the portion of energy that enters the cathode for AISI H13 tool steel. Also in this paper, the effect of EDM parameters on MRR has been investigated by using the technique of design of experiments and response surface methodology. Finally, a quadratic polynomial regression model has been proposed for MRR, and the accuracy of this model has been checked by means of analysis of residuals.

Hinduja, S. et al.,[27]. This paper reviews the models that have been developed to simulate each of these phenomena, e.g. potential models to calculate the current density distribution in ECM, thermal models for the plasma arc in EDM, moving boundary models to simulate the anodic dissolution in ECM and probabilistic models to determine the discharge location in EDM. In addition to discussing the relative merits of the techniques deployed in these models, the paper

describes some salient applications and concludes with desirable future enhancements to these models.

Shao, B. et al.,[28] In this paper, comprehensive electro-thermal model of micro-EDM has been used to simulate the crater formation process is presented. This model incorporates realistic machining conditions such as Gaussian distributed heat flux, temperature dependent thermal properties and expending plasma radius. The heat transfer equation and experimental measurements of a generated crater dimensions are used to determine the energy distribution fraction to the electrodes, a crucial parameter of the micro-EDM modelling. Simulation results show a good agreement with experimental results.

Bao-cheng, X., et al., [29]. In this paper, an axisymmetric three-dimensional thermo-physical model for the electrical discharge machining of titanium alloy was developed using finite element method. To efficiently predict the temperature distribution and the material removal rate, the model considers some realistic parameters such as the plasma channel radius based on discharge current and discharge duration, the latent heat of melting and evaporation, the percentage of discharge energy transferred to the workpiece and Gaussian distribution of heat flux. Numerical simulation of the single spark discharge of titanium alloy machining in electric discharge machining process was carried out using software ANSYS. The effect of various process parameters on temperature distributions along the radius of the workpiece was reported. Finally, the model was validated through EDM experiments, showing that it can efficiently predict material removal rate.

Salah, N.B., et al.,[30] In this paper, numerical study of thermal aspects of electric discharge machining process is done. This paper presents numerical results concerning the temperature distribution due to electric discharge machining process. From these thermal results, the material removal rate and the total roughness are deduced and compared with experimental observations. It is shown that taking into account the temperature variation of conductivity is of crucial importance and gives the better correlations with experimental data.

Assarzadeh, S., et al., [31] In this study, more realistic assumptions including Gaussian type distribution of spark heat flux, temperature dependent materials properties, latent heat of melting and expanding plasma channel with pulse current and time have been made to establish a comprehensive modelling platform. The

ABAQUS FEM software has been used to simulate the mechanism of crater formation due to a single discharge. The non-uniform thermal flux was programmed through the DFLUX subroutine. The simulation results show that the temperature of work piece decreases as the discharge time increases while the volume of melted and evaporated material increases. A specially designed single spark experimental set-up was developed in laboratory to carry out a few single spark tests for verification purposes. The obtained craters morphologies were examined by optical microscopy and scanning profilometer. It has been shown that the present approach outperforms other previously developed thermal models with respect to cavity outline and size possessing the maximum confirmation errors of 18.1% and 14.1% in predicting crater radius and depth, respectively. Parametric analysis reveals that the melting boundary moves onward by increasing discharge current, whereas it moves back prolonging discharge time. Finally, a closer proximity to experimental material removal rates than those predicted by analytical approach has been recognized which confirms its more precise generalization capabilities towards the real state EDM process.

Eubank. T, et. al.,[21] A variable mass, cylindrical plasma model (VMCPM) is developed for sparks created by electrical discharge in a liquid media. The model consists of three differential equations—one each from fluid dynamics, an energy balance, and the radiation equation—combined with a plasma equation of state. A thermo-physical property subroutine allows realistic estimation of plasma enthalpy, mass density, and particle fractions by inclusion of the heats of dissociation and ionization for a plasma created from deionized water. Problems with the zero-time boundary conditions are overcome by an electron balance procedure.

Numerical solution of the model provides plasma radius, temperature, pressure, and mass as a function of pulse time for fixed current, electrode gap, and power fraction remaining in the plasma. Moderately high temperatures (≳5000 K) and pressures (≳4 bar) persist in the sparks even after long pulse times (to∼500 μs). Quantitative proof that superheating is the dominant mechanism for electrical discharge machining (EDM) erosion is thus provided for the first time. Some quantitative inconsistencies developed between our (1) cathode, (2) anode, and (3) plasma models (this series) are discussed with indication as to how they will be

rectified in a fourth article to follow shortly in this journal. While containing over-simplifications, these three models are believed to contain the respective dominant physics of the EDM process but need be brought into numerical consistency for each time increment of the numerical solution.

Oßwald, K., et al., [33] This paper presents a novel method for the detailed experimental analysis of the energy distribution in continuous sinking EDM processes. For this purpose, sophisticated measurement methods for temperatures and electrical quantities were combined. Thus, the experimental setup was very close to realistic process conditions. The results of the obtained temperature profiles and the derived energy distribution are presented followed by variations of process parameters and a critical discussion to explain deviations. This paper presents a novel method for the detailed experimental analysis of the energy distribution in continuous sinking EDM processes. For this purpose, sophisticated measurement methods for temperatures and electrical quantities were combined. Thus, the experimental setup was very close to realistic process conditions. The results of the obtained temperature profiles and the derived energy distribution are presented followed by variations of process parameters and a critical discussion to explain deviations.

Erden, A., et al., [34] This paper summarizes the experimental and theoretical investigations to determine the effect of impurities in dielectric liquid on the electric discharge machining performance. Commercial kerosene is used as the dielectric liquid and, brass-steel and copper-steel pairs are used for machining. Copper, Aluminium, Iron and Carbon powder are added into the dielectric liquid as artificial impurities. Natural contamination of the liquid is also investigated Experiments have shown that impurities improve the breakdown characteristics of the dielectric liquid. Increases in machining rates are obtained by decreased time-lags at high impurity concentrations. Short circuits are observed, at too high impurity concentrations, resulting in decreased machining rates. Surface quality and the gap size are also found to be affected by the impurity concentrations.

Joshi, S.N., et al.,[35] This paper reports an intelligent approach for process modelling and optimization of electric discharge machining (EDM). Physics based process modelling using finite element method (FEM) has been integrated with the soft computing techniques like artificial neural networks (ANN) and genetic

algorithm (GA) to improve prediction accuracy of the model with less dependency on the experimental data. A two-dimensional axi-symmetric numerical (FEM) model of single spark EDM process has been developed based on more realistic assumptions such as Gaussian distribution of heat flux, time and energy dependent spark radius, etc. to predict the shape of crater, material removal rate (MRR) and tool wear rate (TWR). The model is validated using the reported analytical and experimental results. A comprehensive ANN based process model is proposed to establish relation between input process conditions (current, discharge voltage, duty cycle and discharge duration) and the process responses (crater size, MRR and TWR) .The ANN model was trained, tested and tuned by using the data generated from the numerical (FEM) model. It was found to accurately predict EDM process responses for chosen process conditions. The developed ANN process model was used in conjunction with the evolutionary non-dominated sorting genetic algorithm II (NSGA-II) to select optimal process parameters for roughing and finishing operations of EDM. Experimental studies were carried out to verify the process performance for the optimum machining conditions suggested by our approach. The proposed integrated (FEM–ANN–GA) approach was found efficient and robust as the suggested optimum process parameters were found to give the expected optimum performance of the EDM process.

Tlili, A., et al.,[36] Electrical discharge machining (EDM) simulation is proposed in this study through an improved numerical model based on the finite difference method. This model takes into account the growth of the plasma channel and the instantaneous removal of material throughout the electric discharge. The criteria used to assess the validity of the model are the material removal rate and morphology of the crater. The comparison of numerical and experimental results, in the case of the tool steel AISI D2, shows encouraging results.

Jatti, V.S., et al.,[37] Present study focuses on developing Finite Element model of Powder Mixed Electric Discharge Machining of Beryllium copper alloy with experimental validation. An axis symmetric three-dimensional model has been developed and simulated using ANSYS 15.0 software for obtaining the temperature distribution on the surface of workpiece during a single discharge machining process. And the temperature profile was utilized to estimate the material removal rate. Experiments were performed to validate the numerical results. The average

percentage error of 7.8% was obtained between numerical and experimental results. Thus, a good agreement between the experimental and numerical results shows that the software model can efficiently simulate and predict the real time results.

Zhang, Y., et al.,[38] In this paper, a new method of investigation the characteristic of EDM plasma was proposed. The heat flux of the plasma was investigated by comparing the boundary of the melted material in the crater which was obtained by metallographic method and the isothermal surface of the thermal-physical model calculated by finite element method (FEM). The results indicated that the Gauss heat source was much more consistent with the actual EDM process compared with the other heat source type, such as point heat source, circular heat source. The data proposed in this paper can be further used in the existing thermo physical models, expecting to bring the models preciously more close to the actual case.

Shankar, P., et al., [39] In this study, a fundamental study of electro discharge machining (EDM) based on the physics of an arc and heat transfer theory has been carried out. The field equations for electric potential and temperature in the spark region are simultaneously solved by employing the finite element method. Using the criterion of constant current at any cross section of a spark, the arc radii at different cross sections are corrected until convergence. The final spark shape obtained is non-cylindrical, and has different radii at different cross sections. Also, the percent of heat input absorbed by cathode, anode, and dielectric has been calculated. The computed relative electrode wear has been compared with experimental results.

Jeswani, M. L.[40] In this paper effect of the addition of graphite powder to kerosene used as the dielectric fluid in electrical discharge machining is done. Experimental results reveal that the addition of about 4 g of fine graphite powder (10 μm in average size) per litre of kerosene increases the metal removal rate (MRR) by 60% and the tool wear rate (TWR) by 15% in electrical discharge machining. The wear ratio TWR/MRR is reduced by about 28%. This effect may be attributed to the reduction in the breakdown voltage of the kerosene dielectric caused by the addition of the graphite powder. A scheme of in-process measurement of graphite contamination, based on measuring the clarity of the kerosene with a photodiode, is proposed.

Kuneida, M., et al., [41] In this paper, it was showed that electrical discharge machining (EDM) can be achieved in gas can be achieved. With the help of a high-pressure gas flow supplied through a thin-walled pipe electrode, the molten workpiece material can be removed and flushed out of the working gap without being reattached to the electrode surfaces. The greatest advantage of this technique is that the tool electrode wear ratio is almost zero for any pulse duration. Hence a 3D shape can be machined very precisely using a special NC tool path which can supply a uniform high-velocity air flow over the working gap. Furthermore, the material removal rate is improved as the concentration of oxygen in air is increased, due to oxidation of the electrode materials.

Marashi, H., et al.,[42] This article provides a review of dielectric modifications through adding powder to dielectric. Utilizing powder mixed dielectric in the process is called powder mixed EDM (PMEDM). In order to select an appropriate host dielectric for enhancing machining characteristics by adding powder, a brief background is initially provided on the performance of pure dielectrics and their selection criteria for PMEDM application follow by powder mixed dielectric thoroughly review. Research shows that PMEDM facilitates producing parts with predominantly high surface quality. Additionally, some studies indicate that appropriate powder selection increases machining efficiency in terms of material removal rate. Therefore, the role of powder addition in the discharge characteristics and its influence on machining output parameters are explained in detail. Furthermore, by considering the influence of the main thermo-physical properties and concentration of powder particles, the performance of various powder materials is discussed extensively. Since suitable powder selection depends on many factors, such as variations in EDM, machining scale and electrical and non-electrical parameter settings, a thorough comparative review of powder materials is presented to facilitate a deeper insight into powder selection parameters for future studies. Finally, PMEDM research trends, findings, gaps and industrialization difficulties are discussed extensively.

Jahan, MP., et al., [43] This chapter presented a comprehensive overview on the micro-EDM process, its varieties, and important applications of each variety of micro-EDM. The chapter started with a brief overview of the micro-EDM process including the physics of the process, sparking and gap phenomena in micro-EDM,

differences between macro and micro-EDM, and a brief discussion on system components of micro-EDM. An overview of different process parameters (electrical, nonelectrical, materials, and motion control parameters, etc.) and performance measure parameters (micro-EDM erosion efficiency, material removal rate, electrode wear ratio, surface roughness, etc.) has been presented with definition and terminology. A detailed section on different varieties of micro-EDM, their working principle, and related important applications are also presented. Finally, some novel applications of micro-EDM indicating the research advances and development in the area of micro-EDM have been presented.

Chakraborty, S., et al.,[44] This paper presents a a detailed information on the use of dielectric fluids and also their effects in electrical discharge machining characteristics.

Shen, Y., et al.,[45] In this study, a low-flux pump is utilized to supply deionized water at a controlled rate to the high-speed air pipe, which affords a mist dielectric to the machining process. Compared with dry EDM,the high-speed near dry EDM improves the cooling capacity and increases the dielectric strength of the dielectric. Furthermore, electrode injection flushing assisted by side flushing of high-speed mist was used to reduce debris deposition and improve cooling capacity. Comparative milling experiments of Ti6Al4V were conducted under the dry and near dry conditions using the different flushing ways. The effects of current, pressure, droplet size, electrode rotation speed, and droplet density on the material removal rate, surface roughness, width of overcut in continuous machining and material removal weight, trace length, trace width in single pulse machining were studied. In addition, scanning electron microscope, X-ray diffractometer, energy dispersive spectrometer, and micro-hardness tester were also used to study the micro-characters of the machined materials.

Fu Ou, S., et al.,[46] This study focuses on machining orthopedic-implant materials based on titanium and titanium–tantalum alloys using bioactive hydroxyapatite (HA)-powder suspension as the dielectric. The influence of the powder particles and the work-piece composition on the machining performance was investigated. Employing a suspension dielectric with 5 g/L HA caused a smoother surface (Ra 2.1 μm) with a thinner recast layer (~9 μm) as compared to using water to machine titanium which has surface roughness of Ra 2.4 μm with a

recast layer close to 10 μm. In addition, the MRR of titanium machined in the HA-powder-suspension dielectric (6.4×10^{-4} g min^{-1}) was greatly lower than that in water (28.6×10^{-4} g min^{-1}). However, increasing the HA concentration led to a gradual increase in the MRR, electrode wear rate (EWR), surface roughness, and recast-layer thickness. The MRR, EWR, and the surface roughness of titanium and titanium–tantalum alloys inverse relation with respect to the melting temperature and under PMEDM exhibited an thermal conductivity of the alloy. Furthermore, calcium and phosphorus were incorporated into the recast layer, and their amounts decreased when the discharge current was increased.

Govindan, P., et al.,[48] The increased MRR in magnetic field assisted dry EDM (by ~130%) was attributed to several reasons including confinement of plasma due to Lorentz forces. The conjectures were investigated further by undertaking over 100 single-discharge, dry and liquid EDM trials, with and without magnetic fields, by varying current, voltage, magnetic field, pulse on-time and bi-pulse current. The magnetic field assistance increased the depth and reduced crater diameter by 80% in dry EDM; and reduced crater diameter marginally but significantly improved uniformity in the material erosion, in liquid EDM. The role of Lorentz forces in confining plasma and reduction in electron mean free path due to magnetic field, when modelled analytically, captured the experimental trends very well.

Salonitis, K. et al., [47]The die-sinking electrical discharge machining (EDM) process is characterized by slow processing speeds. In this paper, research effort has been focused on optimizing the process parameters so as for the productivity of the process to be increased. In this paper a simple, thermal based model has been developed for the determination of the material removal rate and the average surface roughness achieved as a function of the process parameters. The model predicts that the increase of the discharge current, the arc voltage or the spark duration results in higher material removal rates and coarser workpiece surfaces. On the other hand the decrease of the idling time increases the material removal rate with the additional advantage of achieving slightly better surface roughness values. The model's predictions are compared with experimental results for verifying the approach and present good agreement with them.

Kansal, H.K., et al., [8] In this paper, an axisymmetric two-dimensional model for powder mixed electric discharge machining (PMEDM) has been

developed using the finite element method (FEM). The model utilizes the several important aspects such as temperature sensitive material properties, shape and size of heat source (Gaussian heat distribution), percentage distribution of heat among tool, workpiece and dielectric fluid, pulse on/off time, material ejection efficiency and phase change (enthalpy) etc. to predict the thermal behaviour and material removal mechanism in PMEDM process. The developed model first calculates the temperature distribution in the workpiece material using ANSYS (version 5.4) software and then material removal rate (MRR) is estimated from the temperature profiles. The effect of various process parameters on temperature distributions along the radius and depth of the workpiece has been reported. Finally, the model has been validated by comparing the theoretical MRR with the experimental one obtained from a newly designed experimental setup developed in the laboratory.

Schulze, H.P., et al., [51]The crater morphology has been investigated in different procedures. An analytical relation between pulse parameters and roughness has been achieved and differences between a single discharge and a sequence of discharges are described. Simulations of thermal-affected zones are identified for a single discharge and a sequence of discharges. The characteristics describing the changed gap conditions of the discharge types in the simulation model are shown. Starting from measured current and voltage curves, the thermal channel base parameters are computed.

Apart from this a lot of literature regarding the mechanism of EDM, it's various types (hybridised and non-hybridised), it's different process parameters, their influence on the MRR and surface roughness of the machining process has been also studied thoroughly.

2.3 IDENTIFIED RESEARCH GAPS IN THE LITERATURE

After going through all the literature certain loop-holes or research gaps has been identified. These gaps are listed as follows:

- Absence of effect of time-lag variation in the mathematical modelling of PMND-EDM process.
- No substantial focus on the consideration of metallic powder's characterstic features like their shape and size in the mathematical model. Also, their effect on the MRR has not been investigated analytically.

- Absence of multistep verification of the experimental results. As most of the researchers has used FEM modelling only, to verify the experimental results.
- A lot of research considered a two-dimensional planar model for modelling of machining phenomenon which is not very realistic in nature. In addition to that, most researches had used a two dimensional FEM module viz. ANSYS PARAMETRIC DESIGN LANGUAGE (APDL).
- A very less amount of research has been done with copper and die steel as tool and workpiece material respectively in case of PMND-EDM. Due to this, the curious case of lowering of MRR with a continuous increase on powder concentration has not been investigated thoroughly.

CHAPTER 3

RESEARCH OBJECTIVE

The research gaps that are identified in the previous chapter are taken up the source of motivation for this work. Based upon that, following research objectives were made for this work

- Mathematical modelling of near dry EDM process for material removal using powder particle characteristic.
- Development of 3D FEM model for machining phenomenon of PMND-EDM process using ANSYS WORKBENCH 16.0 module.
- Experimental study on Powder mixed near dry EDM process.

3.1 DEVELOPMENT OF MATHEMATICAL MODEL

In this research, an axisymmetric three-dimensional model for powder mixed electric discharge machining (PMEDM) has been developed using the mathematical modelling method. The model utilizes the several important aspects such as temperature sensitive material properties, shape and size of heat source (Gaussian heat distribution), percentage distribution of heat among tool, workpiece and dielectric fluid, pulse on/off time, material ejection efficiency and phase change (enthalpy) etc. to predict the thermal behaviour and material removal mechanism in PMEDM process.

In PMEDM, a series of rapid, repetitive and randomly distributed discrete electric sparks occur in the gap between tool and work electrodes for a cycle of few microseconds. Addition of powder particles into the dielectric fluid makes this process more complex and random. There had been different kinds of approaches for the analysis of the EDM process. One is mathematical modeling and the other is finite element method (FEM). The thermal part includes all the heat conduction and heat storage. Researchers had attempted analysis in steady state only. Some of them considered unsteady state but they did not developed FEM models of coupled

thermo-electric analysis for EDM process. In this research work, heat transfer mathematical model had been developed for unsteady state. Experiments had been performed on EN-31 steel had been done partially with copper as a tool electrode. Process parameters were current, voltage, powder concentration & pulse on time.

3.1.1 ASSUMPTIONS

This research includes three-dimensional axisymmetric model for PMND-EDM. Mathematical modelling method was used for developing the model. Thermal properties of material, heat source shape (Gaussian heat distribution), heat distribution percentage among workpiece, tool and dielectric fluid, pulse on, pulse off and material ejection efficiency were considered as significant elements for predicting the MRR in PMND-EDM. The following assumptions were considered in order to obtain mathematical feasibility of the problem. Work piece and tool electrodes were assumed to be isotropic and homogenous in nature.

- Properties of the workpiece and tool material were temperature dependent.
- The radius of spark was function of time and discharge current.
- Distribution of heat flux was Gaussian distribution pattern.
- The spark zone was axisymmetric.
- A certain fraction of total spark energy was received by the workpiece.
- Absence of recast layers as the flushing efficiency was assumed to be 100 %.
- Heat transfer mode for transference of heat from plasma to workpiece and electrodes was conduction only.
- The only possible mode of heat transfer between plasma and dielectric fluid was convection. Conduction was considered as chief heat transfer mode between plasma and workpiece.

3.1.2 GOVERNING EQUATION

The governing equation is given by Fourier heat conduction equation:-

$$\frac{1}{r}\frac{\partial}{\partial r}\left(k_t r \frac{dT}{\partial r}\right)+\frac{\partial}{\partial r}\left(k_t \frac{\partial T}{\partial z}\right)=\rho C_p \frac{\partial T}{\partial t} \qquad (3.1)$$

Where T is temperature in kelvin, t is time (s), ρ is density (kg/m$^{3)}$, k_t is thermal conductivity (W/mK), Cp is specific heat capacity of workpiece material (J/Kg k), r and Z depict coordinate axis.

3.1.3 DISTRIBUTION OF HEAT

A Guassian type heat source was considered and it was responsible for heating of the workpiece material. An incident plasma stream was responsible for heating phenomenon. This whole process is depicted clearly Fig.1 [8].

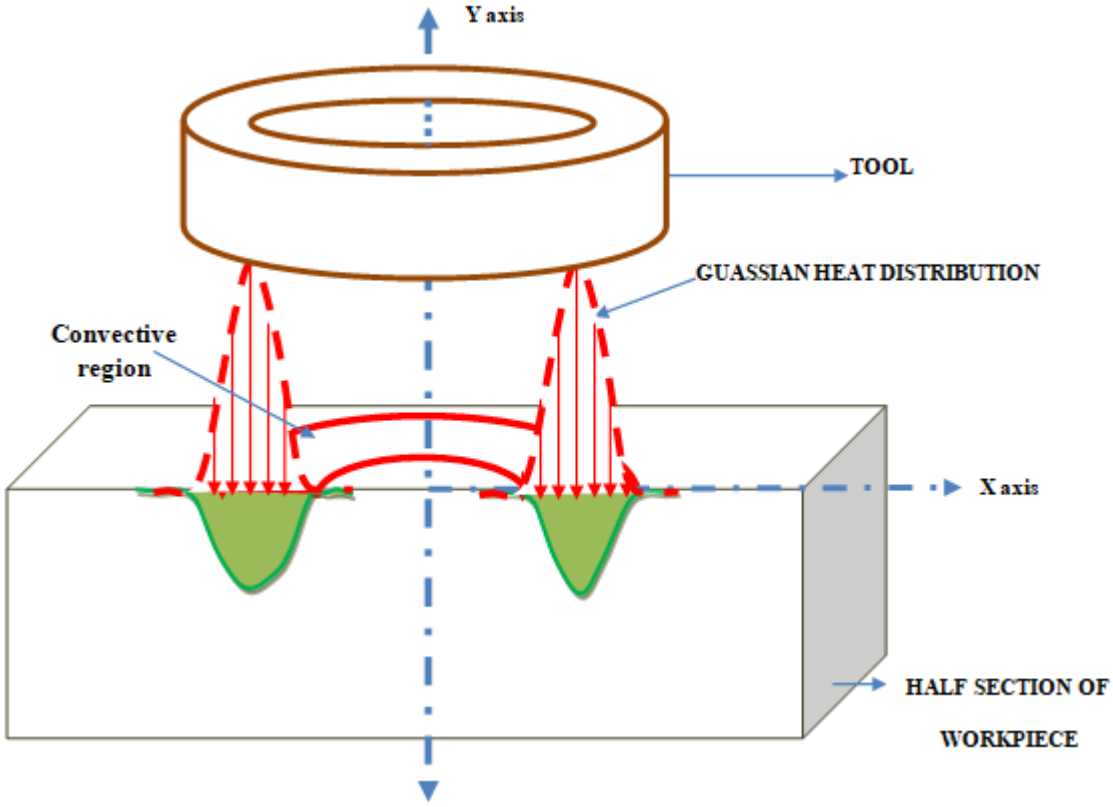

Fig.3.1 Diagram depicting the Gaussian heat distribution in PMND-EDM

3.1.4 BOUNDARY CONDITIONS

A small portion (PQRS) was cut from the workpiece as shown in Fig.2 .Using Gaussian distribution single spark heat spark is applied on the surface of domain (K_1) up to spark radius R.

Heat transfer by convection was applied over the remaining surface of K_1 as cooling effect was provided by powder mixed dielectric fluid. There was no heat transfer on surface boundaries K_3 and K_5 as they were far from spark radius zone. There was no heat transfer at K_4 region because this boundary itself lies at the axis of symmetry.

Boundary conditions for K_1, K_2, K_3, K_4 and K_5 are as follows:

For K_1: $0 \le r \le R$

$$K\frac{\partial T}{\partial z} = q_w(r) \tag{3.2}$$

Beyond spark radius, i.e. $R < r < \infty$:

$$K\frac{\partial T}{\partial z} = h(T - T_o) \tag{3.3}$$

For K_2, K_3, K_4 and K_5:

$$\frac{\partial T}{\partial t} = 0 \text{ (i.e. steady state)} \tag{3.4}$$

where, h is heat transfer coefficient between powder mixed dielectric medium and the surface of the workpiece, heat flux $q_W(r)$ is created due to single spark, T_0 is the initial room temperature and T is the temperature attained after some time.

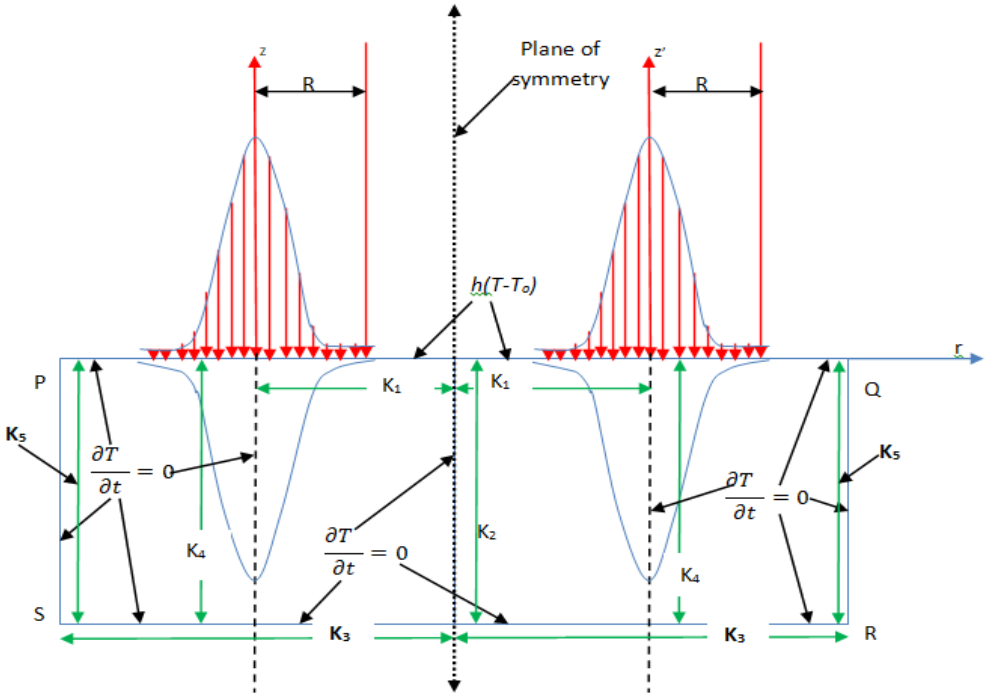

Fig.3.2 Heat distribution pattern for PMND-EDM process.

3.1.5 HEAT INPUT TO WORKPIECE

It was assumed in previous models that all the heat was transferred to the workpiece from the plasma but this approach was not realistic because some percentage of heat was transferred to the dielectric medium and the tool electrodes as well [15, 16]. They revealed by their work that anode and cathode absorbed 8% and 18% respectively and the rest goes to dielectric fluid. It was also proved by researchers that depending on type of dielectric medium and processing time, 40-45% was absorbed by the workpiece [17]. Amount of total thermal energy that was

transferred or conducted to the workpiece or F_c value assumed for this research was 18.3%.

3.1.6 MATERIAL FLUSHING EFFICIENCY

Material flushing efficiency (MFE) was considered to be 100% in earlier models which meant that all the molten removed material from the workpiece was ejected out successfully. But in actual only 10% - 30% was ejected out from the crater [8]. MFE was assumed to be 100% in this present work [9].

3.1.7 HEAT FLUX

Gaussian distribution was used in order to obtain accurate isothermal curves in thermal model for PMND-EDM [18, 19].

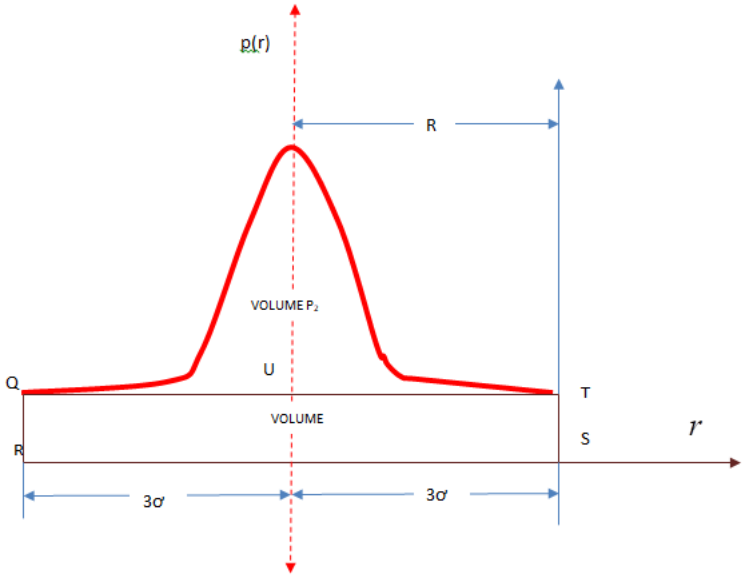

Fig.3 Gaussian distribution for thermal model.

The same effect had been modified into new form by considering the effect of suspended metallic powders in the dielectric medium. A diagrammatical representation of Gaussian heat distribution function is shown in Fig.3 with a random variable ‘ r’ and other relation in Eq.3.5

$$p(r) = \frac{1}{\sqrt{2\pi\sigma}} e^{\frac{-r^2}{2\sigma}} \tag{3.5}$$

Where $\frac{1}{\sqrt{2\pi\sigma}}$ indicated the maximum value that the distribution could attain and σ depicted standard deviation.

Mathematics proves that zero value of Gaussian curve could be possible only when random variable 'r' attained infinity. Due to this reason a definite region on the 'r' axis was considered for depicting the crater's bottom. Standard deviation (σ) varied between (−3σ to and +3σ) thus 99.75% of the values lies within the region (r = μ−3σ and r = μ+3σ) as shown in Fig.3. Three-dimensional representation of the crater can be obtained by giving a complete rotation to the Gaussian curve about the vertical axis.

So, R = 3σ by putting the value of σ into above equation

$$p(r) = \frac{3}{\sqrt{2\pi}\sigma} e^{-4.5\left(\frac{r}{R}\right)^2} \tag{3.6}$$

In PMND-EDM, p(r) refer to the amount of heat energy received by the work surface of the workpiece specimen, shown by q_W and was a function of ' r' Eq 3.14.

At r = 0, p(r) = q_0; (3.7)

Where, q_0 denote the maximum amount of heat energy received at the centre of the work surface of the workpiece specimen. Heat flux of the system is given by Eq 3.8.

$$q_w(r) = q_o e^{-4.5\frac{r^2}{R^2}} \tag{3.8}$$

Thus the energy incident on the workpiece is:

$$\int q_w(r) dA = \int_0^R q_w(r) 2\pi r dr \tag{3.9}$$

$$= -\frac{\pi R^2}{4.5} q_o e^{-4.5\frac{r^2}{R^2}}\Big|_0^R \tag{3.10}$$

$$= 0.2191\pi q_o R^2 \tag{3.11}$$

The rate at which heat energy was incident on the workpiece was identical to the supplied electrical energy rate which was Fc*V*I where, F_c was the fraction of heat input to the workpiece, V_b was the breakdown voltage and I represent the current.

$$F_c V_B I = 0.2191\pi q_o R_c^2 \tag{3.12}$$

$$q_o = \frac{4.57 F_c V_B I}{\pi R_c^2} \tag{3.13}$$

$$q_w(r) = \frac{4.57 F_c V_B I}{\pi R_c^2} e^{-4.5\frac{r^2}{R^2_c}} \tag{3.14}$$

$$Q(t) = \frac{3.4878 \times 10^{5} \times F_C VI^{0.14}}{t_{on}^{0.88}} \left(\exp\left\{ -4.5\left(\frac{t}{t_{on}}\right)^{0.88} \right\} \right) \tag{3.15}$$

$$R_{pc} = \left(2.303e-3\right) I^{0.43} t_{on}^{0.44} \tag{3.16}$$

$$t_B = \frac{6\pi\eta x^2 \ln \gamma_{cr}}{s^2 (E - E_O)^2}. \tag{3.17}$$

$$Q = Q(t) * A \tag{3.18}$$

$$q' = Q * t_B \tag{3.19}$$

$$MRR_d = K_\Phi * q' \tag{3.20}$$

$$MRR = \frac{MRR_d * 60 * 10^{9}}{t_B} \tag{3.21}$$

While calculating heat flux rate through Eq.3.15 expression "*t*" is replaced by t_B as we are considering that whole heat energy in the form of plasma is released within that period of time after complete charging of the capacitor of RC circuit.

Further, t_B *(break down time)* was calculated by including critical concentration ratio. Eq. 3.17 gives a direct relationship between powder concentration and t_B.

In this way the mathematical model for PMND-EDM process is developed. Expression of MRR, heat flux rate and time-lag will be used for calculation of MRR, heat received at workpiece and break-down timing for the machining process.

CHAPTER 4

EXPERIMENTAL SET-UP

4.1 AN INTRODUCTION TO EXPERIMENTAL SET-UP

Indigenous setup for PMND-EDM was developed at Delhi technological university (D.T.U, Delhi) in precision manufacturing lab as shown in Fig.4.1. This setup has advantages in terms of performance enhancements such as increased MRR and production of parts with good surface quality characteristics. This setup had special features such as customized mixing chamber for developing heterogenous dielectric mixture (metallic powder, glycerol and dielectric oil). Precise flow meter was integrated with the setup in order to get the controlled flow rate of the dielectric medium according to required settings for experimentations. Separate provision for controlling the pressure of dielectric mist was provided with the help of manually controlled regulators and valves. A compressor of 2-Hp (Nu-air company made compressor) was used to deliver compressed high pressurized air for dielectric mist formation. Although the working principle in PMND-EDM was same as that of erosion process in EDM, but presence of metallic powder as additives makes the erosion process quite complex. In traditional EDM process the material removal was due to heat erosion or thermo-electric erosion principle, which utilize heat energy in order to melt the metallic workpiece and lead to the formation of crater over the workpiece. Intermittent repetitive sparks were developed at the inter electrode gap (IEG) due to ionization effect when voltage and current is supplied. This interaction between the ions and molecules at IEG leads to formation of high energized plasma which delivered thermal energy over the workpiece from the tool electrode and eventually MRR takes place [21]. But with fusion of metallic powder along with dielectric oil, interlocking phenomenon of powder particles took place which lead to bridge like formation within the dielectric medium [22]. This phenomenon increased the machining gap and reduced the insulating strength of the dielectric medium. Due to this mechanism the plasma obtained was more enlarged and more uniformly

distributed at the machining area which increased the erosion rate and therefore enhanced the MRR. The experiments were conducted on Sparkonix machine (Sparkonix limited, Pune). Dielectric system was responsible for efficient and uninterrupted supply of dielectric medium within the IEG so that essential machining conditions are satisfied during EDM [25]. A multi-phase dielectric fluid composed of kerosene oil, air, stabilizing agent (glycerol) and copper powder at different level of concentration was used.

Effect of various machining parameters such as discharge current, pulse on time, current and voltage were studied on output response which was MRR. The experiments were performed on EN-31 steel as work piece electrode and copper as a tool electrode. Multi-phase dielectric oil has been used as dielectric fluid throughout the tests. The other experimental conditions are shown in Table 4.1.

Table 4.1 Experimental conditions for machining

Workpiece	EN-31
Tool Electrode	COPPER
Dielectric	Air + oil + metallic powder
Discharge Current	12A
Voltage	120 V
Pulse On	10-2000 µs
Pulse Off	125 µs
Polarity	+ve
Powder concentration	2, 4, 6 % (g/l)
Flow rate of dielectric	20 ml/min
Air pressure	0.6 MPa
Oil pressure	0.6 MPa
Powder material	Zinc
Stabilizing agent	Glycerol (5%)

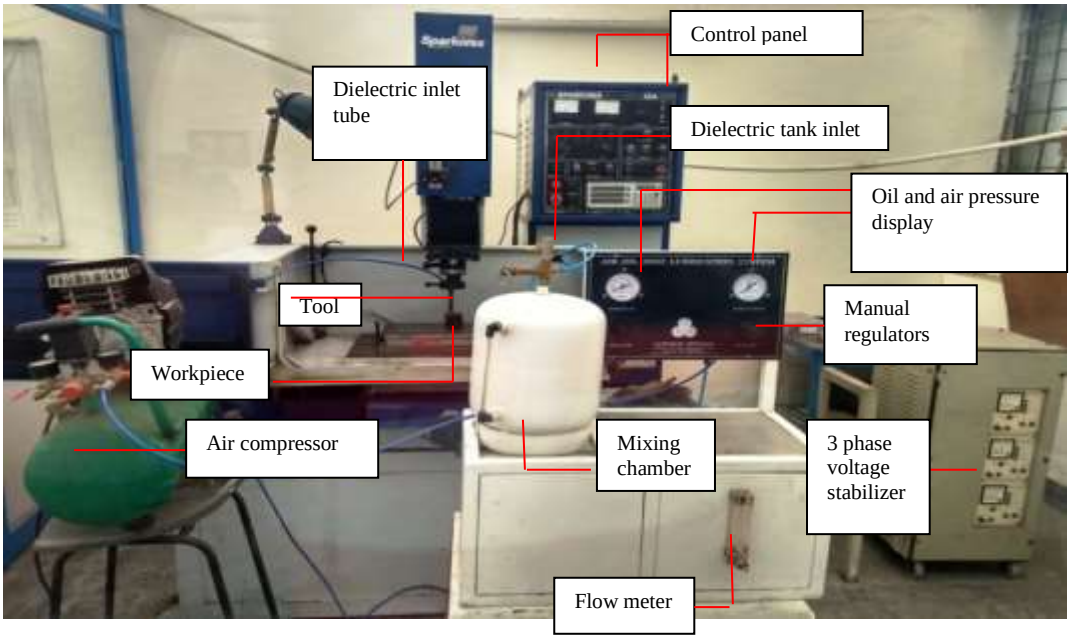

Fig.4.1 PMND-EDM setup developed indigenously for experiments.

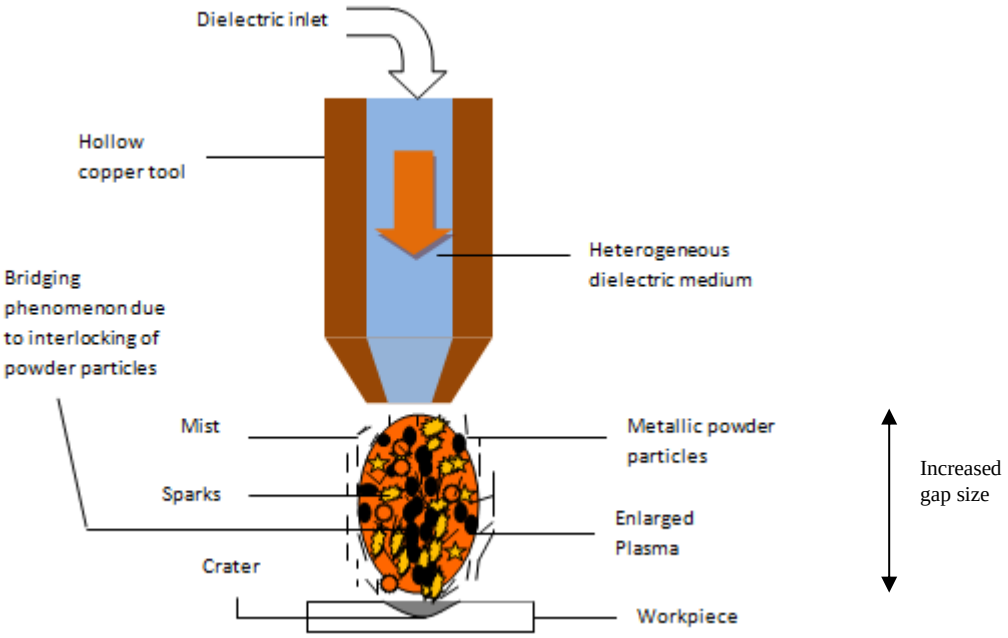

Fig.4.2 Phenomenon of discharge mechanism taking place by energized heat plasma channel in presence of metallic powder as additives.

The work piece material used in this investigation was EN-31 steel. The physical and thermal properties of workpiece electrode materials had been shown in Table 4.2 and Table 4.3. Being a cold work, air hardened tool steel (EN-31) offered high surface hardness and good wear resistance. It was also characterised by its high dimensional stability after hardening and tempering, high compression resistance and

good resistance to tempering. The success of a metal forming tool depends on optimizing all the factors affecting its performance.

Table 4.2 Physical properties of workpiece EN -31.

Properties	Values
Thermal conductivity (W/m*K)	44.5
Hardness(HRC)	63
Yield stress (MPa)	450
Tensile strength (MPa)	750
Density (kg/m^3)	7850
Melting point (^{o}C)	1540

Table 4.3 Chemical composition of workpiece EN-31

Element	%
Carbon	0.90-1.20
Silicon	0.10-0.35
Manganese	0.30-0.75
Sulphur	0.050
Phosphorus	0.050
Chromium	1-1.60

The tool electrode material used in this investigation was copper. Customized hollow tubular copper electrodes were used as tool electrode as shown in Fig. 4.3 and its physical and chemical properties are shown in Table 4.4.

Table 4.4 Physical properties and chemical composition of copper tool electrode.

Properties	Values
Atomic number	29
Atomic weight	63.546
Density (kg/m^3)	8960
Melting point (^{o}C)	1083
Boiling point (^{o}C)	2567
Thermal Conductivity W/m*K	385
Hardness (Mohs)	2.5-3
Tensile strength (MPa)	33.3
Bulk modulus (GPa)	140

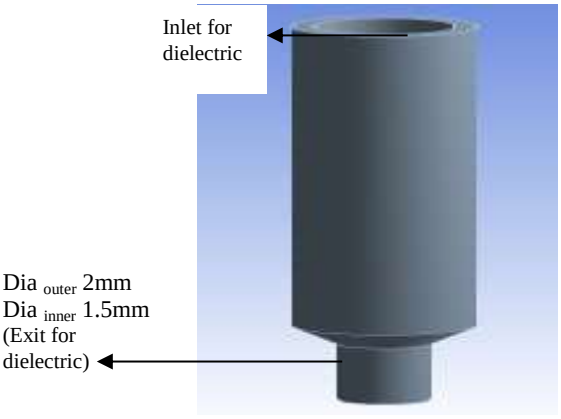

Fig. 4.3 (a) Customized hollow copper electrode

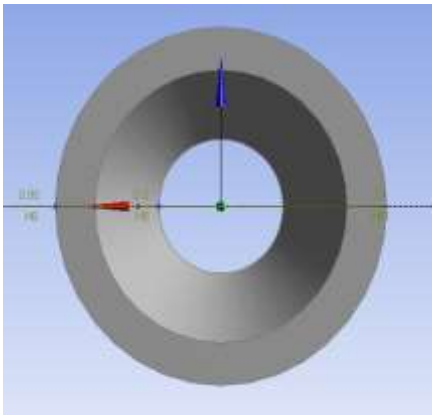

Fig 4.3 (b) Top view of tool electrode

CHAPTER 5

PROCESS PARAMETER SELECTION, EXPERIMENTATION AND CALCULATIONS

In order to attain better machining rates, critical literature survey was done and based on that optimal input parameters considered for study were current, voltage, pulse on time and powder concentration.

MRR was calculated by the formula given below:

$$MRR = (W_i - W_f)/(\rho \times T_m) \quad (5.1)$$

Mass of the specimen was measured using electronic balance of least count 0.001gm (Asia Techno weigh India).

5.1 SCHEME OF EXPERIMENTS

The experiments were conducted according to the given scheme of experiments as shown in Table 5.1 Effect of four parameters was studied for analysis of MRR.

Table 5.1 Process parameters and their levels selected for experimentations.

S. No	Symbol	Process Parameter	Level (Range)	Unit
1	A	Pulse on time	35-500	μs
2	B	Voltage	25V	μs
3	C	Current	12	A
4	D	Powder concentration	2, 4, 6	g/l

Experiments were conducted in three different scenarios as given below.

$I^{st}\ Scenario: V = 25V, I = 12A, \eta = 4.26 * 10^{-3}$ Pa.s, $\gamma_{cr} = 7.8, s = 12.5 * 10^{-3} mm, t_B = 2.334 \mu s.$

$II^{nd}\ Scenario: V = 25V, I = 12A, \eta = 6.89 * 10^{-3}$ Pa.s, $\gamma_{cr} = 1.6, s = 12.5 * 10^{-3} mm, t_B = 0.7213 \mu s.$

$III^{rd}\ Scenario: V = 25V, I = 12A, \eta = 7.231 * 10^{-3}$ Pa.s, $\gamma_{cr} = 6, s = 12.5 * 10^{-3} mm, t_B = 4.469 \mu s.$

5.2 CALCULATIONS

Calculations of heat flux rate, time-lag, material removal per discharge and material removal rate are discussed in following section.

5.2.1 CALCULATIONS FOR TIME-LAG, HEAT FLUX RATE AND MRR FROM THE MATHEMATICAL MODEL

Numerical values of different process parameters like current, voltage, powder concentration and pulse-on timing are used within the derived expressions of time lag (break-down timing), heat flux rate and material removal rate. Additional physical parameters like viscosity, heat transfer coefficient, powder particle radius, electric field intensity, IEG width and average powder concentration. For IInd scenario:

- $\eta = 6.89 * 10^{-3}$ Pas
- $h = 1.259$ W/mm^{2}K
- $s = 12.5*10^{-3}$ mm
- *E-Eo=50-100 V/mm*
- *x= 3mm*
- N_{avg} *=10 g/l*
- N_{cr} *=16 g/l*

$$\text{So } t_B = \frac{6\pi\eta x^2 \ln\gamma_{cr}}{s^2(E-E_O)^2} = \frac{6\pi(0.00629)(0.003)^2 \ln\left(\frac{16}{10}\right)}{\left(\frac{12.5}{1000}\right)^2 (66666.67)^2} = 0.7213\mu s$$

$$Q(t) = \frac{3.4878\times10^5 \times F_C VI^{0.14}}{P_{on}^{0.88}} \left(\exp\left\{ -4.5\left(\frac{t}{P_{on}}\right)^{0.88} \right\} \right) W/mm^2.$$

$$Q(t) = \frac{3.4878\times10^5 * 0.183 * 25 * 12^{0.14}}{0.000035^{0.88}} \left(\exp\left\{ -4.5\left(\frac{0.7213}{0.000035}\right)^{0.88} \right\} \right) W/mm^2$$

$$Q(t) = 16257.3 W/mm^2$$

Using, A= $3.14*(2^2-1.5^2) = 5.497787$ mm^2

Now by using values of Q(t), value of area, A from above into the Eq 3.21 we will get

$$MRR = \frac{MRR_d * 60 * 10^9}{t_B}$$

$MRR = 8.824 mm^3 / \min$

5.2.2 CALCULATION OF EXPERIMENTAL MRR FOR THE SAME SETS OF PROCESS PARAMETERS VALUES

- $N_{avg} = 10\ g/l$
- $V = 25V$
- $I = 12\text{A}$
- $Pon = 35\ \mu s$
- $W_i = 57.2397\ g$
- $W_f = 57.17812\ g$
- $Tm = 10$ minutes

Putting above values in eqn 5.1 we will get,

$MRR = (57.2397 - 57.1782)/(0.007850 \times 10)\ \text{mm}^3/\text{min}.$

$MRR = 0.784\ \text{mm}^3/\text{min}.$

Similarly calculations for other case are done and the following results are obtained

Table 5.1 Experimental Results of Response Characteristic for 1st scenario of experiments:

s.no	P_{on} (10^{-6}s)	q (W/mm^2)	MRR (mm^3/min)	Exp MRR (mm^3/min)
1	500	1743.9	0.988	0.919
2	200	3717	2.106	1.686
3	65	8950.4	4.774	3.867
4	35	12439	7.444	4.8576

Table 5.2 Experimental Results of Response Characteristic for 2nd scenario of experiments.

s.no	P_{on} (10^{-6}s)	q (W/mm^2)	MRR (mm^3/min)	Exp MRR (mm^3/min)
1	500	1789.5	0.98	0.784
2	200	3937.7	2.047	1.263
3	65	10033.0	5.4447	4.573
4	35	16257.3	8.824	7.677

Table 5.3 Experimental Results of Response Characteristic for 3rd scenario of experiments.

s.no	P_{on} (10^{-6}s)	q (W/mm^2)	MRR (mm^3/min)	Exp MRR (mm^3/min)
1	500	1691.4	0.284	0.2016
2	200	3468.79	0.3297	0.2605
3	65	7134.6	0.678	0.556
4	35	8885.35	0.858	0.7293

CHAPTER 6

FEM MODELLING AND SIMULATION

6.1 INTRODUCTION

The EDM is a complex thermal erosion process. It involves a great deal of heat transfer in it. The inclusion of metallic powder and stabilising agent in dielectric further increase the complexity of the resulting hybrid EDM process i.e. PMND-EDM process. Understanding of this kind of complexity is not possible merely through mathematical modelling therefore use of FEM techniques is must here. That's why in this work ANSYS Workbench 16.1 has been used for modelling and simulation of the given transient analysis problem. This chapter deals with all aspects of FEM modelling and simulation used throughout this work.

6.2 FINITE ELEMENT ANALYSIS (FEA)

The acronym FEA stands for finite element analysis. At its basis, FEA is a numerical method used to solve engineering field problems by dividing a domain into several smaller finite subdomains, which each act as individual elements over which algebraic equations are applied and an approximate solution is given using the finite difference method. The results from each finite element are then reassembled and different types of analysis can be run to solve any number of complicated engineering problems using this method and a powerful solver.

The basic method by which a problem is solved using FEA can be broken down into several steps. First, the problem must be identified and classified. There are several different types of analysis that can be performed. Selecting the correct analysis for the correct problem is important. Next, a simplified mathematical model should be derived from which to build the basic physical concepts of the analysis. Preliminary analysis is then performed, in which a solution is obtained to help ballpark the result sought after from the FEA study. The next step is to actually perform the finite element analysis, which is almost always done with the aid of a

computer. The final step is to check the results. It is important to first note if the results “look” correct, if they make sense, and if they are similar to the preliminary analysis performed. It may also be necessary to check the results against other solution forms, or against a physical model. It must also be noted that the FEA process is a very iterative one. Revisions are often needed after interpreting the results of a study.

The actual FEA portion of the solution method described above can be broken down into eight steps, many of which are typically performed by a computer. The first step is to break the system into “finite elements” by discretizing the system into several elements formed by associated nodes. There are a variety of different types and shapes of elements available for use, depending on the geometry of the system. The second step is to select a displacement function to fit each element. The strain-displacement and stress-strain relationships are then selected in the third step, which is dependent on the material properties of each element. Fourth, the stiffness matrix equations are derived by the computer, and fifth, they are assembled into a global matrix with all elements and boundary conditions incorporated. Sixth, the equations are solved simultaneously to determine the displacement at each node. Consequently, the seventh step is to then calculate the stress and strain for each element using the relationships determined before the equation assembly. Finally, the eighth step is to interpret the results, a vague but important task that will be discussed in more detail late. This method is a general one, and there are multiple ways that it is implemented in different FEA computer programs.

On a larger scale, the method can be broken down into pre-processing, numerical analysis, and post-processing. Pre-processing refers to all the data input by the user related to the geometry, material properties, element types and mesh, loads, supports, boundary conditions, etc. The numerical solution step is then performed by a computer. This step was broken down into parts above, and consists of the processor combining the equations into matrix form and then solving simultaneously. Finally, post-processing occurs, in which the results are displayed in graphical form. The information is automatically generated once requested by the user.

The use of FEA provides several advantages over other solution and modelling methods. First, by dividing a system into small parts, systems with complex geometries or several materials can be easily represented in one model. This

provides a huge advantage over traditional analysis methods and allows engineers to solve unique problems which would have required much simplification years ago. The size of the elements can also be varied throughout the model to increase or decrease resolution in areas that need to be more closely examined or are not important to the result. Additionally, the method can handle general load conditions and an unlimited number and types of boundary conditions. The method can also handle a large variety of problems, including heat transfer, stress analysis, dynamic problems, and nonlinear problems.

The current section provides the basics and terminological familiarisation of FEA as used in the current study.

6.2.1 GENERATION OF GEOMETRICAL MODEL

At first the translation of physical model into the FEA model has been done. A geometric model of PMND-EDM workpiece electrode has been generated using nodes and elements. In Ansys software, we can develop the geometry within the same module or we can import it from some other module or CAD software. In general simple geometry like this model can be developed within the Ansys Design Modeler software very easily.

6.2.2 TYPES OF FEM MODELS

Finite element models comprises point elements, line elements, area elements, or solid elements.

- **Line Models**: these types of models are used to depict the two or three dimensional structures of beams and cylinders, three dimensional axis-symmetric shell structures. They are mostly developed directly.
- **Two dimensional solid analysis models**: Used for featuring thin planar structures or axis-symmetric solid structures in 2-D space. They are generated through solid modelling, generally.
- **Three dimensional shell models**: Used for featuring thin structures in 3-D space and are generated through solid modelling.

- **Axis-symmetric models**: they are symmetric about on particular axis or centre axis. Cones, straight cylinders, spherical, hemispherical shapes and discs are some examples of these models.

6.2.3 SELECTION OF ELEMENT TYPE

A continuum has to be discredited into basic finite elements. Thus, the finite elements are geometrically simple so as to accurately model the arbitrary shape into finite elements. The element dimensionally should be in sync with the continuum dimensionally. The main types of elements in FEM are as follows :

- **One dimensional elements** : Two most popular types of one dimensional element are truss and beam elements which are generally used in solid mechanics. Both of them have 2-node (linear), 3-node (quadratic) and 4-node(cubic).
- **Two dimensional elements**: These are of two types, viz. triangular (linear, quadratic and cubic) and quadrilateral (linear, quadratic and cubic). Triangular elements mostly in use are 3-node and 10-node, whereas, Quadrilateral elements have minimum of 4 and maximum of 12-nodes.
- **Three dimensional elements**: These are further of three types, viz. Tetrahedral (linear, quadratic and cubic), Prism (linear, quadratic and cubic) and Hexahedral (linear, Quadratic and cubic).

A number of FEA packages are available for the design purpose. The elements supported by a specific package are called its element library. In the element library of ANSYS, two types of elements are available, namely. Area and volume elements which are further of linear and quadratic types.

6.2.4 CO-ORDINATE SYSTEMS

Geometrical objects may be located by the global and local coordinate systems. It is simpler and easier to define the coordinates in a system rather than in global Cartesian. When a node or a key-point is to be defined, it’s coordinatedds are interpreted in the global Cartesian system. The Ansys software accepts the input of geometry in any of the three pre-defined global coordinate systems available to suit the different conditions.

Following section is listing various types of coordinate systems.

- Global coordinate system
- Local coordinate system
- Display coordinate system
- Nodal coordinate system
- Element coordinate system
- Result coordinate system

6.2.5 MESHING OF MODELS

Being the most important stage of FEM analysis, the decision taken here will be going to effect the accuracy, preciseness and economic viability of the analysis. This part deals with the development of a meshed model of already developed geometrical model by adopting suitable meshing element and appropriate meshing methodology.

6.2.5.1 PROCEDURE FOR MESHING OF MODELS

The procedure for meshing a geometrical model is described as:

- Defining the element attributes
- Setting the mesh controls
- Generation of the mesh

6.2.5.2 SELECTION OF APPROPRIATE MESH DENSITY

The mesh density is of utmost importance during the meshing of model. If the mesh is too course, it may cause serious errors in results. If mesh is too fine, then it may promote long run time on the computer. To overcome these problems, proper selection of mesh density is required. The following procedure has been adopted to select density of mesh in modelling:

- Adaptive meshing should be employed for generating a mesh that meets acceptable energy error estimate criteria. This technique is used for linear static structural or steady state problems.

- Comparison of results of preliminary analysis with independently derived experimental or analytical results.
- Requirement of refinement of mesh in regions where the discrepancy between known and calculated result is too high.
- Re-analyse the problem using twice as many elements in the critical region and compare both of the solutions. If both of the meshes yields different results, then further mesh refinement might be required. And if not the convergence condition has been achieved and programmer must use the last element size for further process.

6.3 APPLICATION OF FEM IN THERMAL MODELLING

For PMEDM analysis, the heat conduction Eq. (3.1) is required to be converted into FEM form and can be written in differential form as:

$$\rho Cp\left(\frac{\partial T}{\partial t}\right)+(L)^{T}\left(Q_{p}\right)=0 \tag{6.1}$$

Where

ρ = density, C_p = specific heat, T = Temperature, t = time, (L) = vector operator and

Q_p = heat flux operator.

$$\{L\}=\begin{Bmatrix}\frac{\partial}{\partial r}\\ \frac{1}{r}\frac{\partial}{\partial \theta}\\ \frac{\partial}{\partial z}\end{Bmatrix}$$

$$\{Q_p\}=\begin{Bmatrix}Q_r\\ Q_\theta\\ Q_z\end{Bmatrix}$$

In order to simplify the analysis, the presented model has been made axisymmetric by reducing the final model to two dimensional. In this light, the vector operator and the heat flux vector has been redefined as

$$\{L\} = \begin{Bmatrix} \frac{\partial}{\partial r} \\ \frac{\partial}{\partial z} \end{Bmatrix}$$

$$\{Q_p\} = \begin{Bmatrix} Q_r \\ Q_z \end{Bmatrix}$$

The variable T depends upon the space and time and has been rewritten as eq 6.2

$$T = \{N\}^T \{T_E\} \tag{6.2}$$

Where,

$\{N\}$ = Element shape function

$\{T_E\}$ = Element's nodal temperature vector

The derivative of eq 6.2 w.r.t time may be written as eq 6.3

$$\frac{\partial T}{\partial t} = T = \{N\}^T \{T_e\} \tag{6.3}$$

Combining $\{L\}$ with T, the expression for temperature, T, has been reduced to eq 6.4:

$$\{L\}T = [\mathrm{B}]\{T_e\} \tag{6.4}$$

Where,

[B] = shape function derivative matrix evaluated as integration points

$$= \{L\}\{N\}^T \tag{6.4.1}$$

Let δT be the small change in the temperature at the node. The δT may be written in the same form as of T as

$$\delta T = \delta T_e^T \{N\}$$

Now, the variation statement has come out to be eq 6.5:

$$\int_V \rho C_P \{\delta T_e\}^T \{N\}\{N\}^T \{\dot{T}\} + \int_V \{\delta T_e\}^T \{B\}^T [K]\,[B][T_e] dV$$

$$= \int_{\exists_b} \{\delta T_e\}^T \{N\} Q_p \, d\dot{\exists}_b + \int_{\exists_{b1}} \{\delta T_e\}^T \{N\} h(T - \{N\}^T \{\delta T_e\}) d\exists_{b1} \quad (6.5)$$

Where, [K] is conductivity matrix, h = heat transfer coefficient,]b is the boundary of domain element $\dot{T}e$ *and* $\{\delta T_e\}$ are nodal quantities which do not vary.

In eq 6.5, all the quantities are seem to be multiplied by the arbitrary vector $\{\delta T_e\}^T$, this term can be dropped from resulting equation. Thus eq 6.5 reduces to :

$$\rho \int_V C_P \{N\}\{N\}^T \{\dot{T}_e\} dV + \int_V [B]^T [K] [B] \{T_e\} dV$$

$$= \int_{\exists_b} \{N\} Q_p \, d\dot{\exists}_b + \int_{\exists_{b1}} \{N\} h(T - \{N\}^T \{\delta T_e\}) d\exists_{b1} \quad (6.6)$$

The eq 6.6 can be written in final assembled finite element form as:

$$\left[C_{p_e}\right]\left\{\dot{T}_e\right\} + \left([K_e^d]\right)\{T_e\} = \{Q_e\} + \{Q_e^c\} \quad (6.7)$$

Where,

$\left[C_{p_e}\right] = \rho \int_V C_P \{N\}\{N\}^T dV =$ Elemental capacitance (specific heat) matrix

$\left[K_e^d\right] = \int_V [B]^T [K] [B] dV$ = Elemental diffusion conductivity matrix

$\{Q_e\} = \int_{\exists_b} \{N\} Q_p \, d\dot{\exists}_b$ = Element mass flux matrix

$\{Q_e^c\} = \int_{\exists_{b1}} Th\{N\} d\exists_{b1}$ = Element convection surface heat flow vector.

The differential form of eq 6.7 can be interpreted as:

$$[C_G]\left\{\dot{T}_G\right\} + ([K_G])\{T_G\} = \{Q_G\} \quad (6.8)$$

Where,

$[C_G]$ = Global capacitance (specific heat) matrix

$[K_G]$ = Global conductivity matrix

$[Q_G]$ = Global heat flux vector

$[T_G]$ = Global temperature vector

$[\dot{T}_G]$ = Time derivative of T_G

Eq 6.7 is matrix equivalent of governing equation. The standard solver of Ansys program is used for finding its solutions.

6.4 FINITE ELEMENT MODEL OF PMND-EDM

In modeling a 3-D, 10 node tetrahedral axis-symmetric thermal solid element (SOLID87) was used for discretization of the continuum. Property like thermal conductivity which was temperature sensitive under the category of non-linear material properties was taken into the consideration. A very fine meshing was employed for building a precise and accurate FEM model. Elemental size of 0.03 mm was considered for the development of model. This optimized size was established by testing of vigorous convergence condition at 1, 0.5, 0.2, 0.15, 0.1, 0.015, 0.05, 0.04, 0.035 and 0.03 mm respectively. It was observed that the convergence condition was satisfied within 0.075-0.03 mm and further miniaturization or diminishment of the element size was not giving the correct and justified results of temperature within the given time frame. A total of 7346748 nodes and 5019982 elements were there in the given meshed geometry. An additional refinement of conduction region at the level of 3 (highest level) was purposefully done to obtain smallest possible element. This satisfying convergence condition ensures accurate interpolation of temperature values over that particular region. Due to this fine temperature isotherms were obtained within that region and this region was most prone for deformation due to high temperature assisted erosion.

Steps followed during FEM modelling of the given problem are as follows:

- Aim: Aim of this analysis was solely to obtain the different sets of temperature isotherms over the workpiece during the machining.
- Use of ANSYS mechanical enterprise product.
- Application of transient thermal analysis.

- Problem domain: Here, geometry of the workpiece was developed on Ansys Design Modeler. The geometry of the workpiece was axis-symmetric about z-axis. The dimensional specification of the workpiece were 30mm*15mm*15mm. Apart from that it was ensured that S.I units were right from geometric modelling to transient analysis.

A meshed model of the given workpiece is shown in Fig.6.2.This problem was solved by providing the calculated heat load value (eq.3.15) at the specified spark location. The time steps used for the problem are sum of P_{on} and P_{off}. Here, four different sets of P_{on} viz. 500, 200, 65 and 35μs were used with a constant P_{off} value of 125μs.

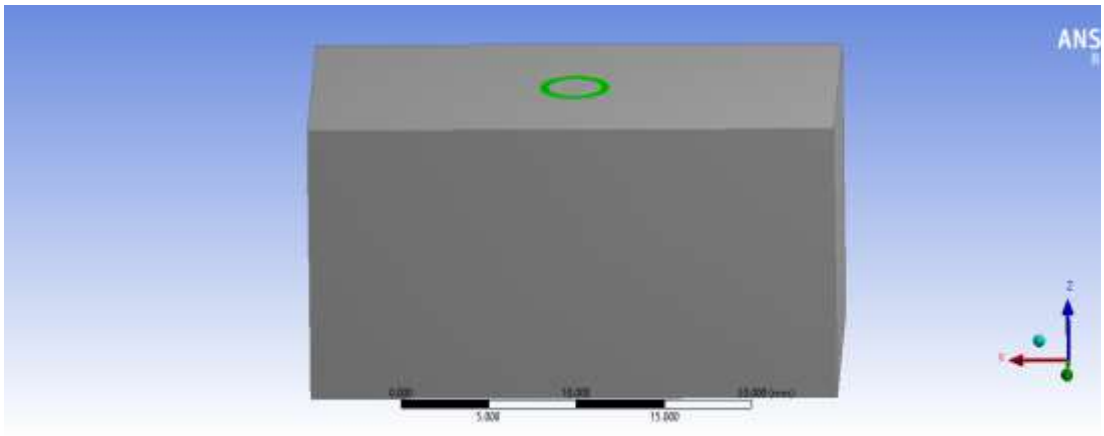

Fig.6.1 A 3-D model of workpiece

Fig.6.2 A 3-D meshed model of workpiece

The following procedure is used for solving the given transient thermal analysis problem of PMND-EDM process on Ansys Mechanical module.

- At first, the meshing of the model with a 0.03mm edge length 3-d, 10 node, tetrahedral element (SOLID87) is performed. Fine meshing of annular region (in which heat flux was applied) is also done at 3 refinement scale. For

obtaining continuous mesh through out the body face meshing tool is applied to all the faces.

- After this settings within the transient thermal menu of model tree are done. Firstly, the initial temperature was set-up at 25^0C. Then, in analyasis settings step end time value is inserted (this corresponds to pulse-on time). After that convection, thermal insulation and heat flux boundary conditions are inserted in the model.
- Now in the solution menu, the location on the workpiece are specified for the different kinds of physical parameters that have to be determined like temperature isotherms along a path, edge, across a face and all over the workpiece.

In this way the the temperature distribution are determined A typical temperature isotherm obtain during the FEM analysis is shown in fig 6.3. From these results temperature value at particular point on the workpiece is determined and these coordinate values are used for material removal calculations, which is discussed in next section.

Fig.6.3 Typical temperature isotherm obtained during FEM analysis of PMND-EDM process with red zone showing the heat affected zone.

6.5 MRR ESTIMATION USING RESULTS OF FEM MODEL

- Different temperature isotherms obtained after transient thermal analysis were used for investigation of amount of workpiece metal machined from the surface of the workpiece.

- A region (area) was estimated as the deformed/eroded region within the sets of different temperature isotherms. The temperature of the isotherms were greater than the melting point of the workpiece material or perhaps more than 60-70^{0}C than melting point (conservatively). At these isotherms various nodes positions were determined which were further used to calculate the eroded material volume during machining.
- Material removal calculation due to single spark discharge was done by calculating the volume of semi-toroidal shape obtained after machining of workpiece (region within which conduction has taken place). This semi-toroidal shape was further divided into numerous cylindrical discs as shown in Fig.6.4. The x, y and z coordinates of the node boundary generated by transient analysis were used for calculating the crater volume.

Total crater volume $V_{vt} = \Sigma_{p=o}^{n} j_i$.. (6.9)

Where

$$j_i = \pi(R_i^2 - r_i^2) * \left|(Z_o - Z_i)\right|.. \quad (6.10)$$

Furthermore, MRR was given by

$$MRR = \frac{60 * V_{vt}}{P_{on} + P_{off}} (mm^3 / \min). \quad (6.11)$$

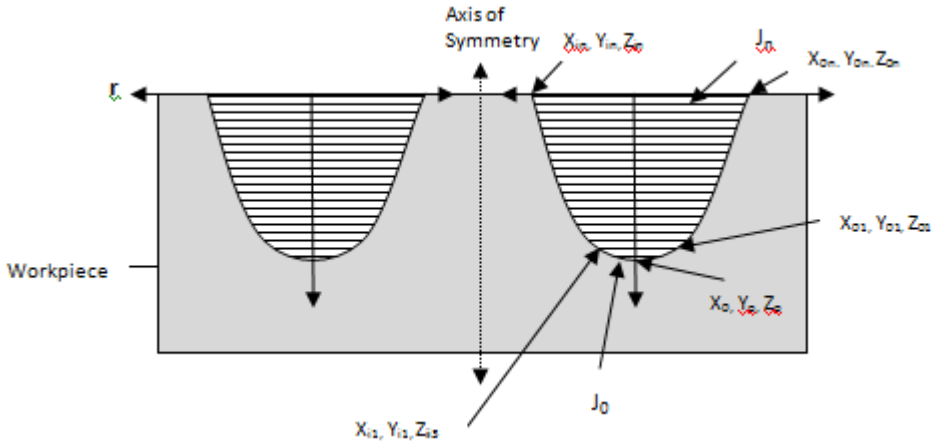

Fig.6.4.Volume measurement method of a semi-toroidal crater.

CHAPTER 7

RESULTS, THEIR ANALYSIS AND DISCUSSION

7.1 INTRODUCTION

This chapter is focused upon the documentation of results obtained from experimentation, analytical modelling and FEM simulation. Then analysis of these results is carried out in a thorough way.

7.2 RESULTS

- **Data used:**

I^{st} *Scenario* : $V = 25V, I = 12A, \eta = 4.26 * 10^{-3}$ Pa.s,$\gamma_{cr} = 7.8, N_{\infty} = 5g/l, s = 12.5 * 10^{-3} mm, t_B = 2.334\mu s.$

II^{nd} *Scenario* : $V = 25V, I = 12A, \eta = 6.89 * 10^{-3}$ Pa.s,$\gamma_{cr} = 1.6, N_{\infty} = 10g/l, s = 12.5 * 10^{-3} mm, t_B = 0.7213\mu s.$

III^{rd} *Scenario* : $V = 25V, I = 12A, \eta = 7.231 * 10^{-3}$ Pa.s,$\gamma_{cr} = 6, N_{\infty} = 15g/l, s = 12.5 * 10^{-3} mm, t_B = 4.469\mu s.$

Table 7.1 Experimental Results of Response Characteristic for 1st scenario of experiments:

s.no	P_{on} (10^{-6}s)	q (W/mm^2)	MRR (mm^3/min)	Exp MRR (mm^3/min)	FEM MRR (mm^3/min)
1	500	1743.9	0.988	0.919	1.34339
2	200	3717	2.106	1.686	2.316494
3	65	8950.4	4.774	3.867	4.552085
4	35	12439	7.444	4.8576	6.287056

Table 7.2 Experimental Results of Response Characteristic for 2nd scenario of experiments.

s.no	P_{on} (10^{-6}s)	q (W/mm^2)	MRR (mm^3/min)	Exp MRR (mm^3/min)	FEM MRR (mm^3/min)
1	500	1789.5	0.98	0.784	2.664837

2	200	3937.7	2.047	1.263	2.501906
3	65	10033.0	5.4447	4.573	5.726975
4	35	16257.3	8.824	7.677	9.76989

Table 7.3 Experimental Results of Response Characteristic for 3rd scenario of experiments.

s.no	P_{on} (10^{-6}s)	q (W/mm^2)	MRR (mm^3/min)	Exp MRR (mm^3/min)	FEM MRR (mm^3/min)
1	500	1691.4	0.284	0.2016	1.570494
2	200	3468.79	0.3297	0.2605	2.096792
3	65	7134.6	0.678	0.556	3.939678
4	35	8885.35	0.858	0.7293	4.311583

7.3 ANALYSIS OF RESULTS OBTAINED THROUGH FEA SIMULATION.

Results obtained from FEM modelling actually were in terms of set of temperature isotherms at different levels of time steps (i.e at different values of P_{on}). A different set of temperature isotherms were obtained at each powder concentration ratio level. From these isotherms variation in size of deformed region was clearly indicated. This could be checked by taking co-ordinates of extreme nodal points in each case. This meant that due to decrease in *Pon* the arc/plasma size was increasing (radially).The deformation region was decreasing as the powder concentration level had gone beyond 5 i.e at 10 and 15. This fact suggests that as powder concentration in dielectric was helping in widening of discharge channel due to increased level of conduction during machining. Temperature isotherms for each case of powder concentration and different pulse-on timing are shown in following figures.

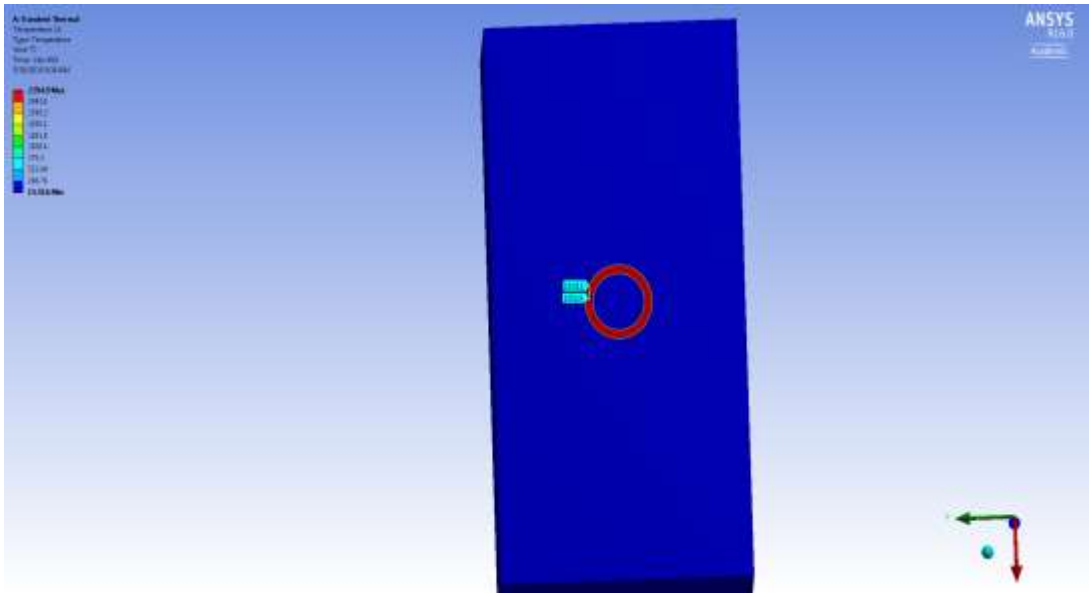

Fig. 7.1 Temperature distribution at heat flux value 1691.1W/mm^2 corresponding to N_∞ = 15 g/l at 500µs pulse-on time.

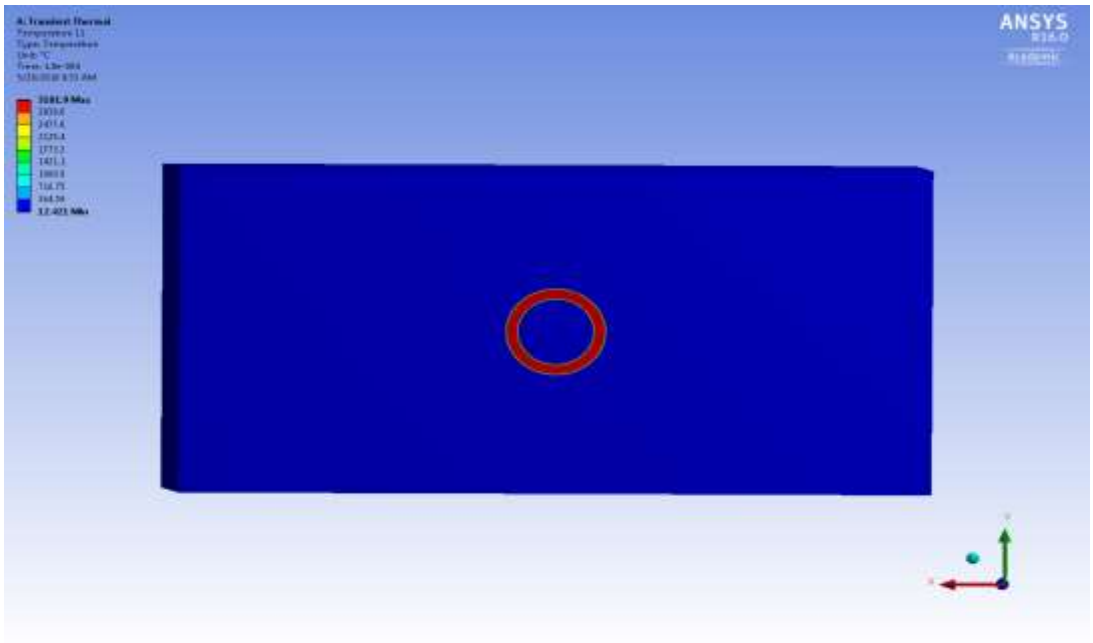

Fig. 7.2 Temperature distribution at heat flux value 8590W/mm^2 corresponding to N_∞ = 5 g/l at 65µs pulse-on time.

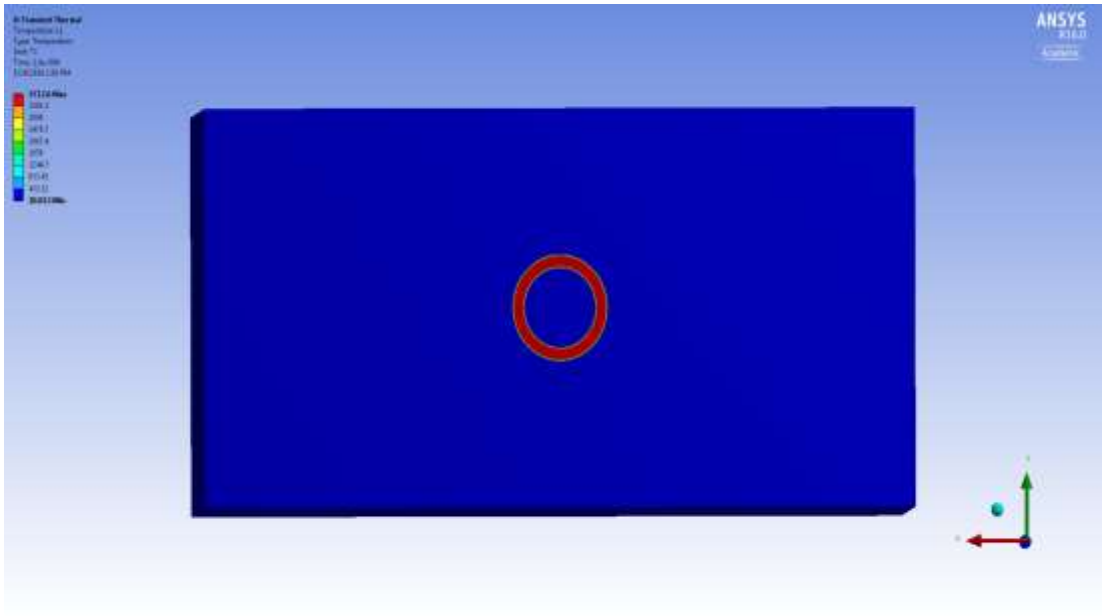

Fig. 7.3 Temperature distribution at heat flux value 10033.3 W/mm^2 corresponding to N_∞ = 10 g/l at 65μs pulse-on time.

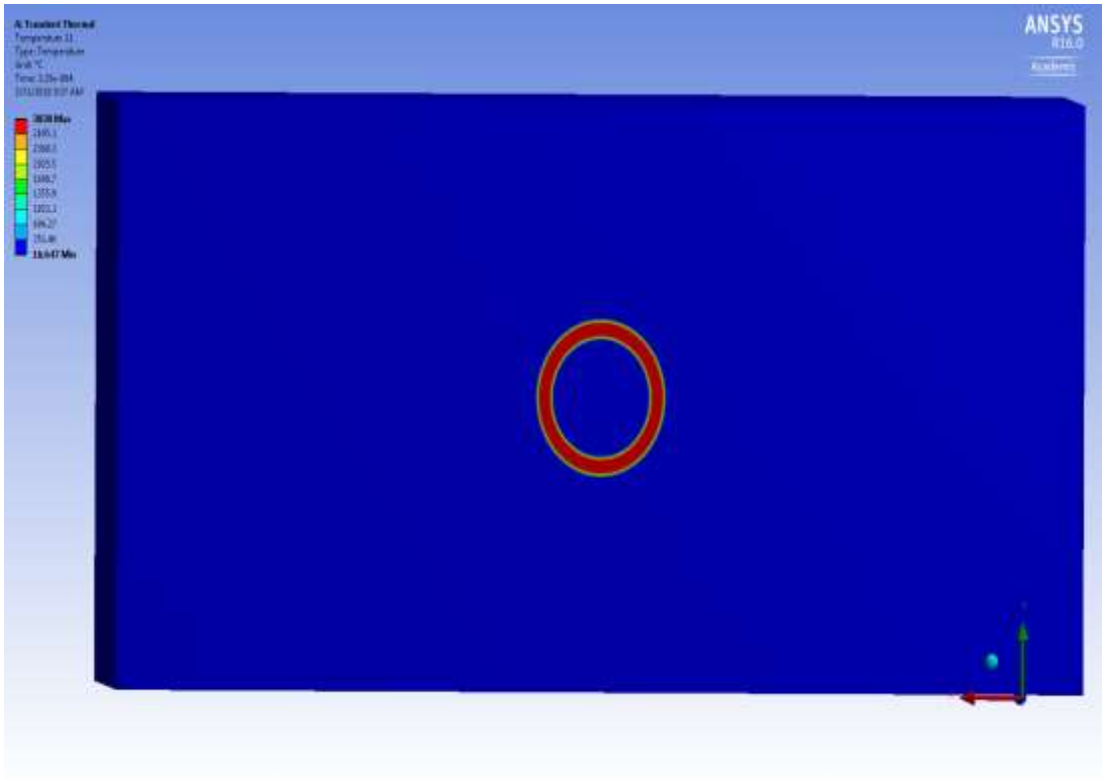

Fig. 7.4 Temperature distribution at heat flux value 3937.7 W/mm^2 corresponding to N_∞ = 10 g/l at 200μs pulse-on time.

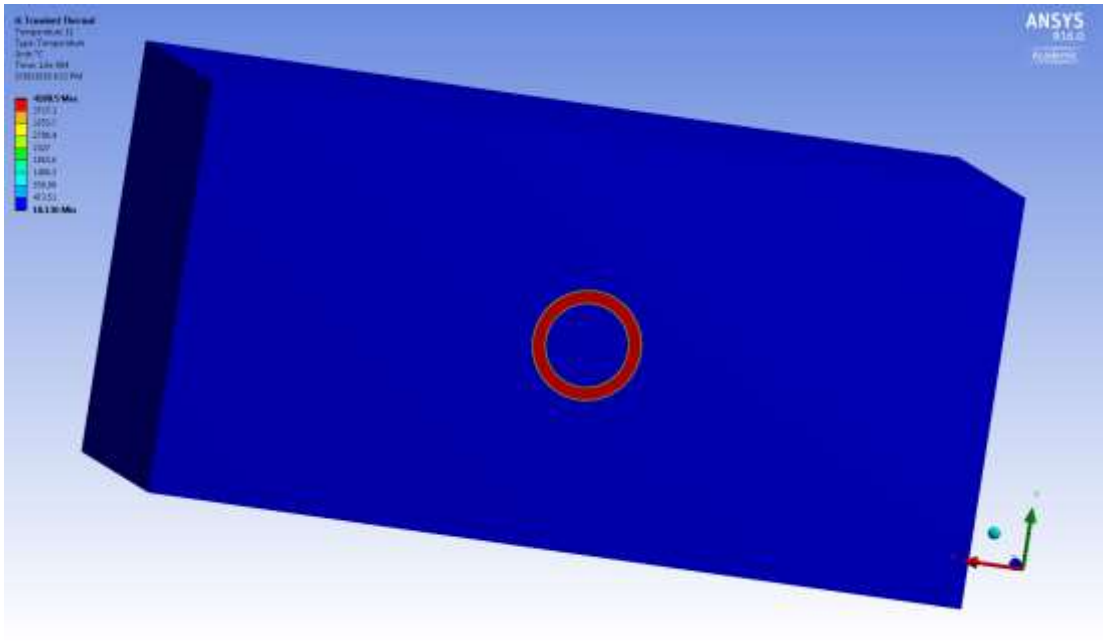

Fig. 7.5 Temperature distribution at heat flux value 16257.3 W/mm^2 corresponding to N_∞ = 10 g/l at 35μs pulse-on time.

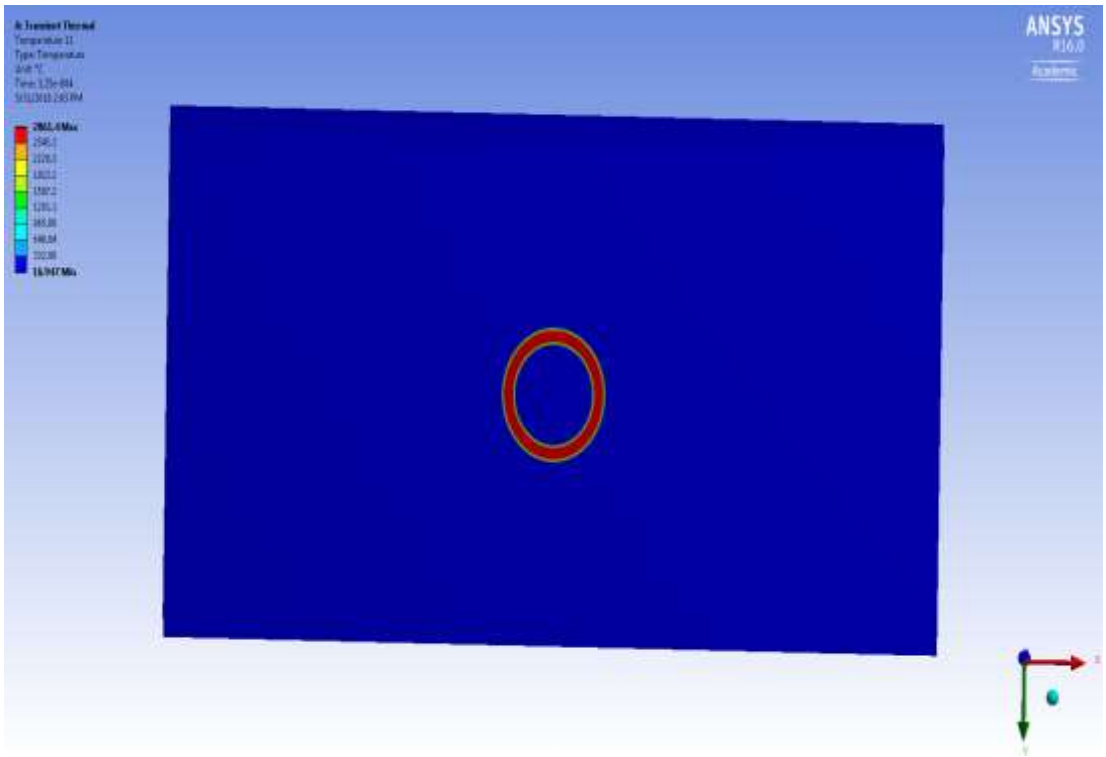

Fig. 7.6 Temperature distribution at heat flux value 3717 W/mm^2 corresponding to N_∞ = 5 g/l at 200μs pulse-on time.

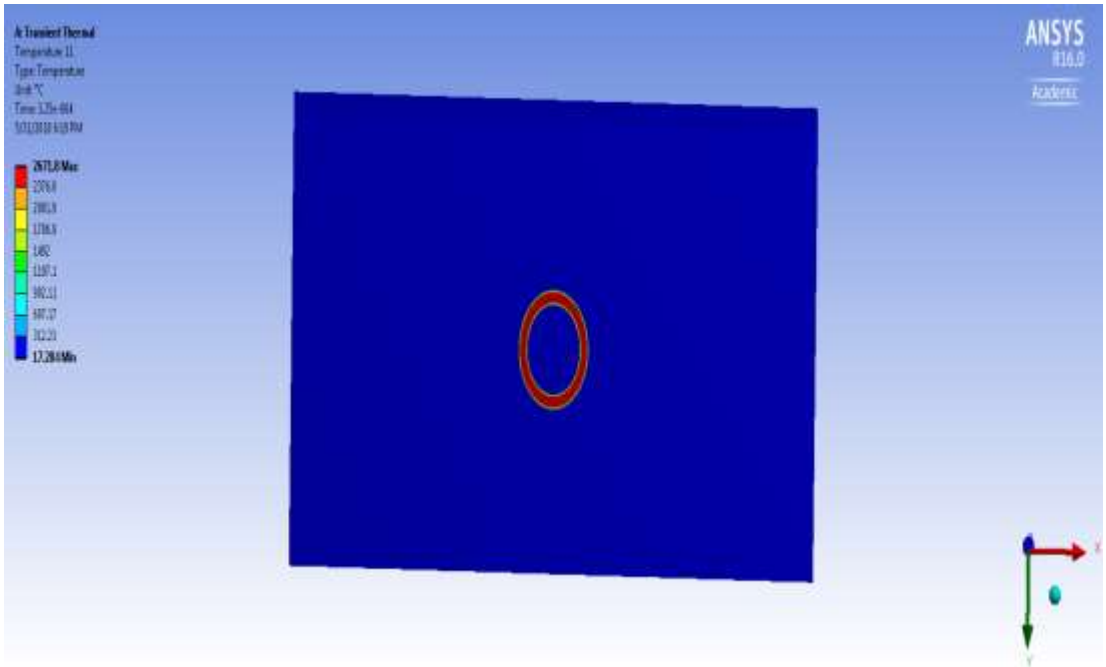

Fig. 7.7 Temperature distribution at heat flux value 3468.8 W/mm^2 corresponding to N_∞ = 15 g/l at 200μs pulse-on time.

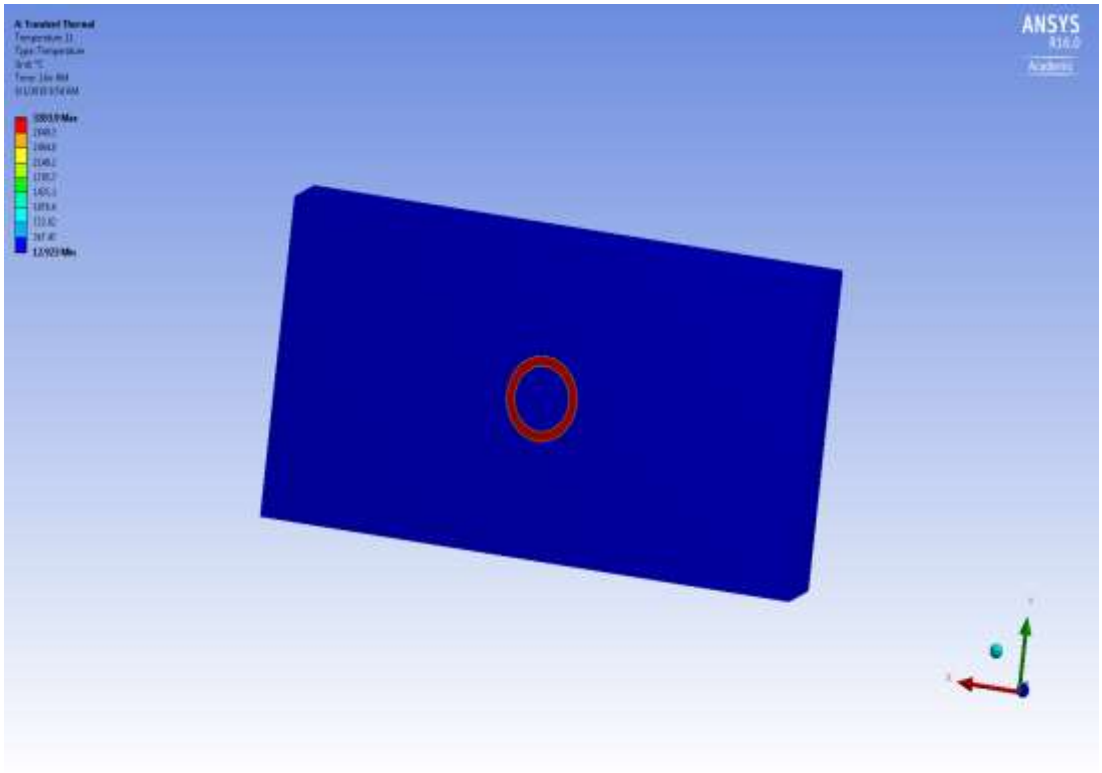

Fig. 7.8 Temperature distribution at heat flux value 12439 W/mm^2 corresponding to N_∞ = 5 g/l at 35μs pulse-on time.

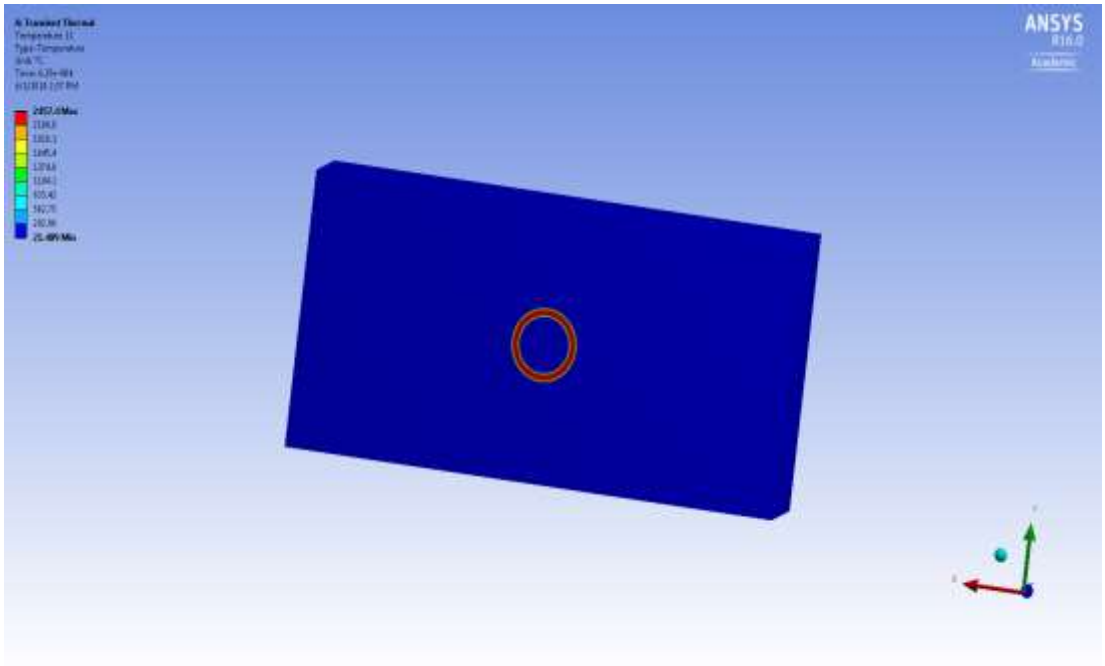

Fig. 7.9 Temperature distribution at heat flux value 1789.5 W/mm^2 corresponding to N_∞ = 10 g/l at 500μs pulse-on time.

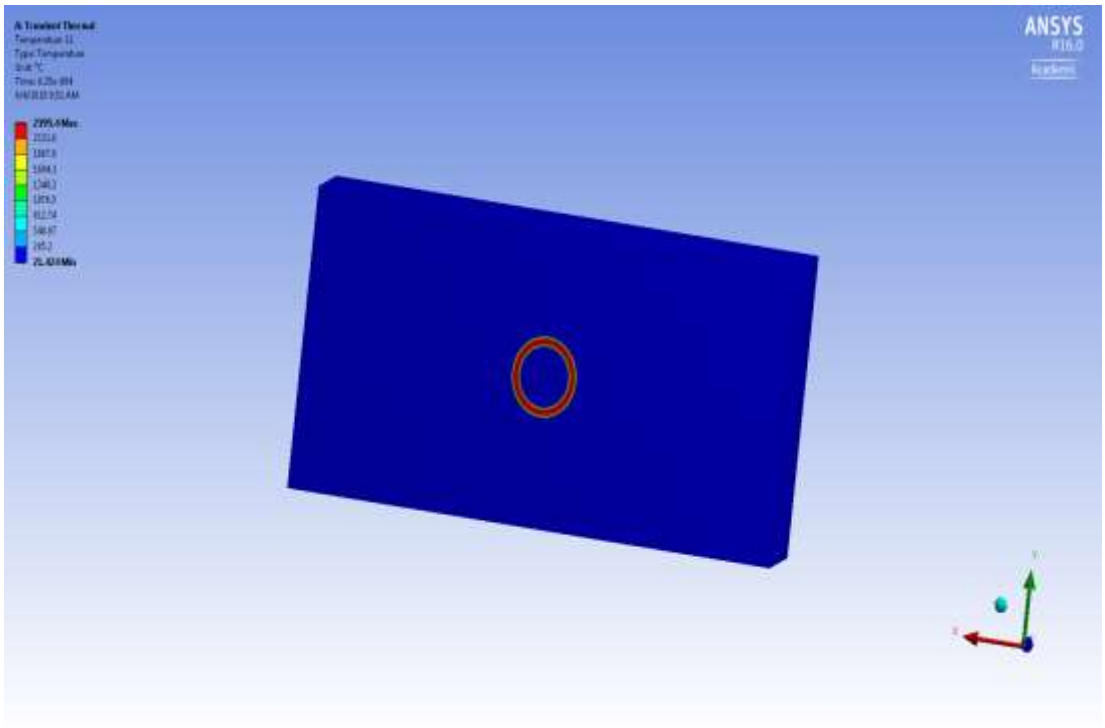

Fig. 7.10 Temperature distribution at heat flux value 1743.9 W/mm^2 corresponding to N_∞ = 5 g/l at 500μs pulse-on time.

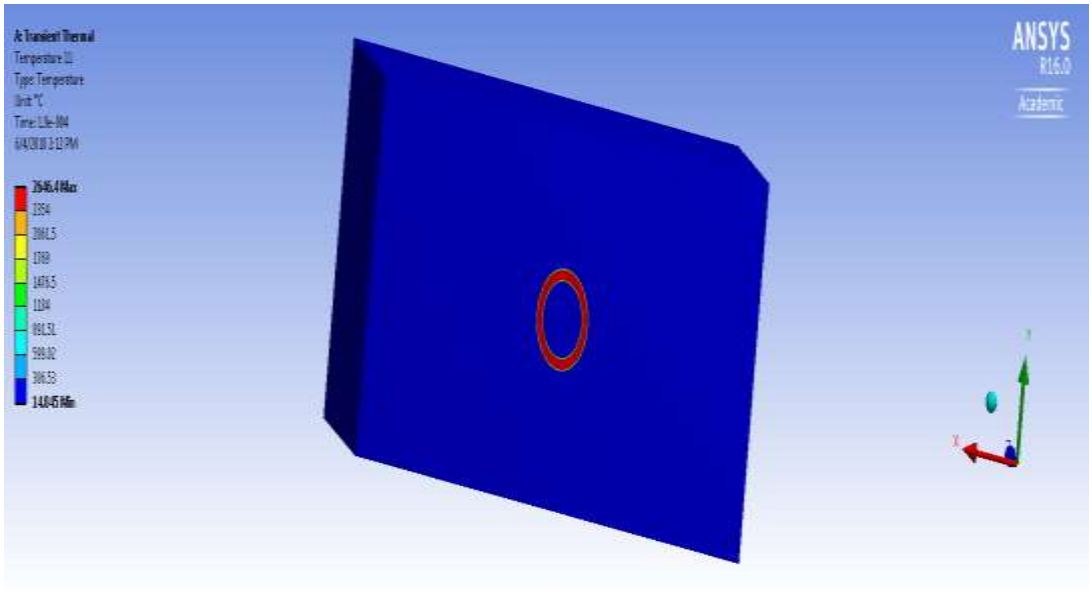

Fig. 7.11 Temperature distribution at heat flux value 7134.6 W/mm^2 corresponding to N_∞ = 15 g/l at 65µs pulse-on time.

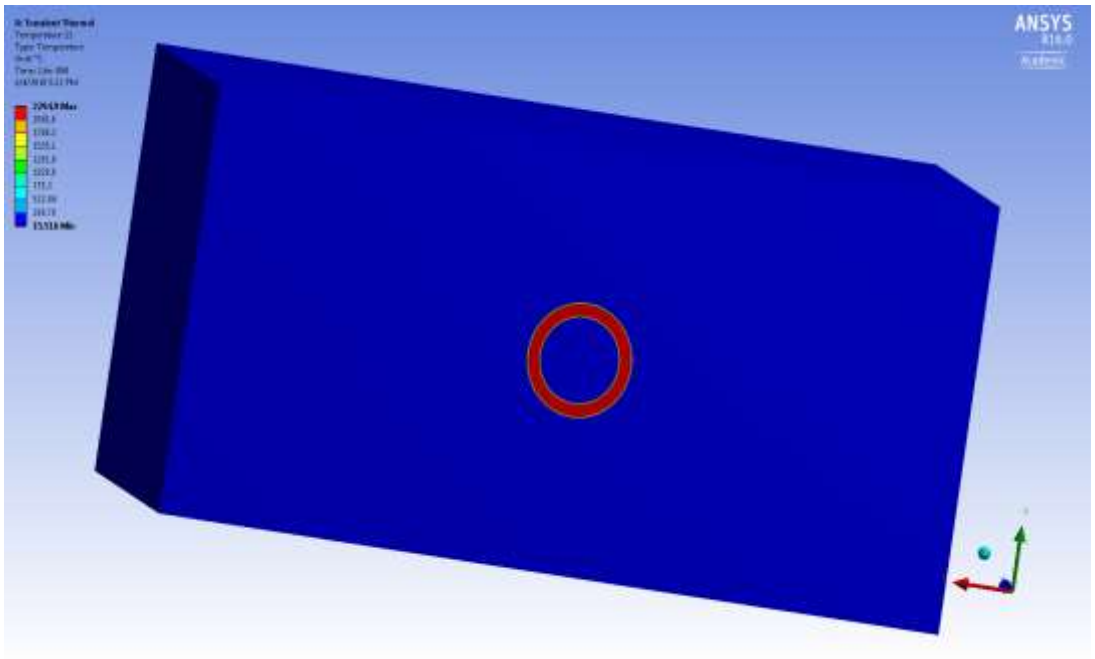

Fig. 7.12 Temperature distribution at heat flux value 8885.4 W/mm^2 corresponding to N_∞ = 15 g/l at 35µs pulse-on time.

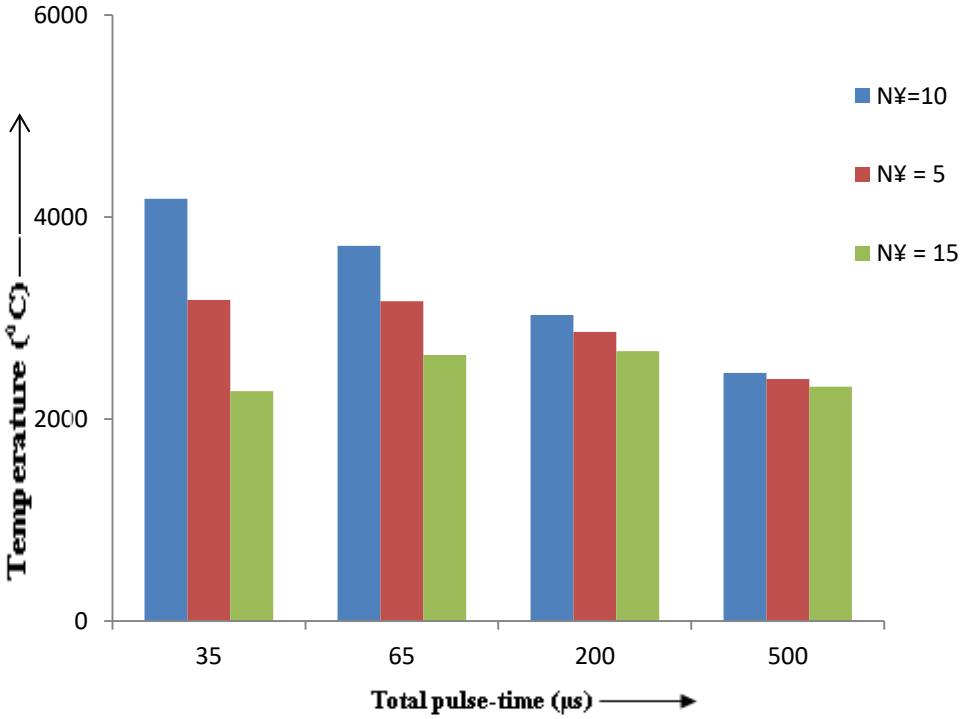

Fig. 7.13 Temperature distribution at various pulse on time values corresponding to various N_{∞} values.

7.4 DISCUSSION OF RESULTS

Results obtained from FEM modeling actually were in terms of set of temperature isotherms at different levels of time steps (i.e at different values of P_{on}). A different set of temperature isotherms were obtained at each powder concentration ratio level. From these isotherms variation in size of deformed region was clearly indicated. This could be checked by taking co-ordinates of extreme nodal points in each case. This meant that due to decrease in *Pon* the arc/plasma size was increasing (radially).The deformation region was decreasing as the powder concentration level had gone beyond 5 i.e at 10 and 15. This fact suggests that as powder concentration in dielectric was helping in widening of discharge channel due to increased level of conduction during machining. But too much increase in concentration level was causing haphazard flow of heat over the workpiece which ultimately lead to loss of most of the heat received by the workpiece.

After obtaining the experimental, theoretical and FEM results at all the three scenarios, comparative study was conducted by means of graph plotted between P_{on} and MRR at three different powder concentrations for all methods respectively.

It was observed that there was a decrease and then increase in the value of t_B with increase of N_∞ value because of inconsistent increase in powder's critical concentration level. The inconsistent increase in powder concentration level was by brought an increase in the inter-electrode gap. This increase in gap had actually eclipsed the effect of increase in conduction of heat energy (caused due to bridging-action of metallic powder) between the tool and workpiece. Other important factor like increase in viscosity also makes this fact stronger. This removed material's location was clearly depicted by the red annular region on the workpiece as shown in Fig. 7.1-7.12. Maximum temperature attained while machining at different pulse-on time values is shown in Fig. 7.13.

Since metallic powder was used in PMND-EDM, a comparatively high degree of conduction takes place within the workpiece. Due to this, heat gets distributed to a larger area of the workpiece as compare to traditional EDM process in the presence of same levels of process parameters used (current, voltage and pulse-on time).

The effect of variation of MRR with respect to pulse-on time and powder's critical concentration ratio is explained later.

7.4.1 EFFECT OF PULSE-ON TIME ON MRR

The volume of material removal was increased with decrease in pulse-on time. This reason attributed to this phenomenon was due to decrease in pulse on time the heat supplied to the workpiece increased as more number of discharge takes place in this condition. Hence larger volume of the workpiece received temperature more than it's melting point (Fig.7.14).

7.4.2 INFLUENCE OF POWDER'S CONCENTRATION LEVEL (N_∞) ON MRR

It was seen that as the value of N_∞ increased from 5 to 15, the heat supplied to the workpiece firstly increased and then decreased due to which volume of material removal got increased and then decreased respectively. This was due to the fact that improper arcing occured as the critical concentration value increased (due to increase in concentration of metallic powder in the dielectric medium). It was observed that very large changes in MRR were absent as the powder concentration

was raised. This was also because for copper and steel combination (as tool and workpiece respectively), the time-lag did not vary for a large extent as the occurrence of short and open circuits was not very frequent in this case [12]. This small variations in time-lag value had only brought small increase in net amount of heat delivered to the workpiece which results in small increment in MRR value as N_∞ increased from 5 to 10. But after N_∞ =10 powder concentration increased so much that haphazard flow of heat takes place within the IEG. As a result of which a considerable amount of heat was lost to the surroundings and workpiece received a lesser amount of heat. And, a comparatively constricted (smaller in area) deformation zone was estabilised which results in reduction of MRR.

So whether we increase the powder concentration from 5 to 15, only a meagre change in time-lag would be observed.

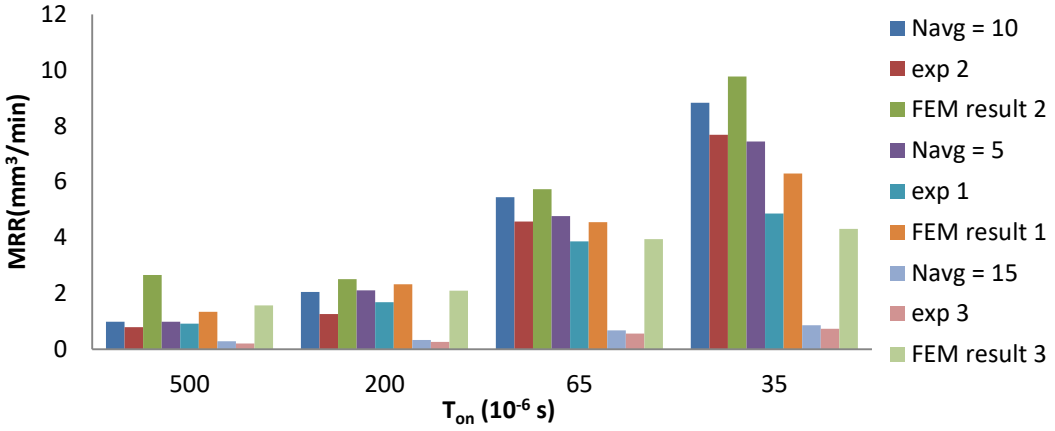

Fig.7.14 Graph between MRR and pulse-on time with different metallic powder concentration.

It was clearly ruled out by the graphs study that the MRR was very low for higher ranges of P_{on} but there was increasing trend in MRR as the P_{on} duration was decreased further. The MRR was maximum in scenario 2nd followed by 1st and 3rd respectively as shown in Fig.14.

7.5 MODEL VALIDATION

The proposed FEM model was validated through experimental and analytical modelling results. MRR values calculated from analytical modelling (Eq. 3.16 – 3.18) and experimental results (through Eq. 3.22) were compared. MRR value was obtained by studying the temperature distribution of FEM model (Eq. 3.19-3.21).

Data regarding this comparison was shown in Table 7.1, 7.2 and 7.3. Based upon these values graph for each case was plotted (Fig. 7.14).

It was seen that the gap between the tool and the workpiece required for spark initiation was increased due to the presence of metallic powder particles if machining was carried out within a voltage range of 80-320 V, provided with electric field intensity of the order of 10^5-10^7 V/m [8]. This resulted in increase in the rate of conduction of heat between the tool and workpiece. This increase in conduction rate was attributed to bridging action of the powder particles within the dielectric medium. As a result short circuiting takes place easily and due to this reason an early explosion of spark was initiated. In addition to this, reduction in pulse-on time increases the frequency of discharges within the circuit which ultimately lead to evolution of heat in a huge amount. Furthermore, lesser amount of fumes were formed during this process due to presence of dielectric oil in minute quantity. PMND-EDM process proved to be more eco-friendlier than normal PM-EDM or traditional EDM process.

CHAPTER 8

CONCLUSION AND FUTURE SCOPE OF THE RESEARCH

8.1 CONCLUSION

In this work, numerical and FEM model of the PMND-EDM process was developed. Here, a 3-D axis-symmetric thermal model of the whole PMND-EDM process was developed on ANSYS Workbench 16.0. The FEM model was used to depict an exact picture of actual PMND-EDM process. In FEM modelling transient thermal analysis of the given model was performed.

From the developed thermo-physical model following observations were made:-

- The heat flux transferred to the workpiece from the tool was a function of breakdown time, pulse-on time, current, voltage and flushing efficiency.
- The break down timing on the other hand depended upon the value of electric field intensity, inter electrode gap (IEG) size, viscosity of multi-phase dielectric, size of metallic powder particles suspended in the dielectric medium and the critical concentration ratio of the powder mixture.
- The value of constant $K_{Ø}$, used in analytical MRR (Eq. 20) depends upon the critical concentration ratio, voltage, current, tool, workpiece and the powder material.
- Further the effect of change in the level of process parameters like pulse on time and critical concentration ratio on material removal rate was investigated. It was observed that MRR value decreased continuously with increase in powder concentration within the dielectric mixture.
- The effect of decrease in the value of pulse-on time resulted in increase of MRR. This material removal or erosion was the result of distribution of those temperature isotherms whose values were greater than the melting point of the work material.

- A striking similarity between the values of experimental work, numerical model and FEM model has been observed in this paper.
- For combination of copper and steel as tool and workpiece material, increase in powder concentration level could not brought increase in MRR every time. Actually, firstly it brought a small increase in MRR but after some concentration levels it got reduced.

8.2 FUTURE SCOPE OF THIS WORK

Since a huge amount of work regarding analytical modeling and FEM modelling has been done in this research work, this same approach of Gaussian distribution of heat can be used for modeling other hybrid EDM processes like PMND-EDM under cryogenic conditions.

This work can be utilised further for determination of residual stresses developed during machining, development of surface cracks, for determination of the surface finish and variation in the properties of dielectric medium while machining.

REFERENCES

1. V.K.Jain, Advanced Machining Processes, Allied Publishers Ltd.,New Delhi, 2002, pp. 126-177.
2. H.Singh, “Experimental study of distribution of energy during EDM process for utilization in thermal models”, Int. J. Heat Mass Transfer , Vol.55 (19) , 2012, pp. 5053– 5064.
3. S.Z. Chavoshi, X. Luo, “Hybrid micro-machining processes: A review”. Precision Engineering, 41, 2015, pp. 1-23.
4. N.Taniguchi, “Current Status in and Future Trends of Ultraprecision Machining and Ultrafine Materials Processing”, Annals CIRP, Vol. 32, No. 2, 1983, pp. 1 -8.
5. J. Marafona, J.G. Chousal, “A finite element model of EDM based on the Joule effect”. Int. J. Machine Tools Manufacturing. 46 (6), 2006,pp. 595–602.
6. F.S. Van Dijck, W.L. Dutre, “Heat conduction model for the calculation of the volume of molten metal in electric discharges [discharge machining]”. J. Phys. D (Appl. Phys.) 7 (6), 1974, pp. 899–910.
7. Koshy Philip, “Electrical Discharge Diamond Grinding: Mechanism of Material Removal and Modeling”, Ph. D. Thesis, I.I.T. Kanpur (India), 1996.
8. H. K. Kansal, S. Singh, P. Kumar, “Numerical simulation of powder mixed electric discharge machining (PMEDM) using finite element method”. Mathematical and Computer Modeling, 47(11-12), 2008, pp. 1217-37.
9. S.N. Joshi, S.S.Pandey, “Thermo-physical modelling of die-sinking EDM process”, Journal of Manufacturing Processes 12, 2010, pp. 45–56.
10. SH.Yeo, W. Kurnia, P.C. Tan, “Critical assessment and numerical comparison of electro-thermal models in EDM”. Journal of Material Processing Technology, 203, 2007, pp. 241-51.
11. R..Snoeys, F.S.Van Dijck, “Investigation of electro-discharge machining operations by means of thermo-mathematical model”. CIRP Ann. 20 (1), 1971, pp. 35–37.

12. A. Erden, S. Bilgin, “Role of impurities in electric discharge machining”, Proc. 21st Int. Machine Tool Design and Research Conference, Macmillan, London, 1980, pp. 345–350.
13. F.S.Van Dijck, W.L. Dutre, “Heat conduction model for the calculation of the volume of molten metal in electric discharges [discharge machining]”. J. Phys. D (Appl. Phys.) 7 (6), 1974, pp. 899–910.
14. S.T.Jilani, P.C.Pandey, “Analysis and modelling of EDM parameters”. Precision Eng. 4 (4), 1982, pp. 215–221.
15. D. DiBitonto, P.Eubank, M. R Patel and M. A. Barrufet, “Theoretical Models of the Electrical Discharge Machining Process—I: A Simple Cathode Erosion Model”, J. Appl. Phys., 66(9), 1989, pp. 4095–4103.
16. H. R. F. Shahri, R. Mahdavinejad, , M. Ashjaee and A. Abdullah, “A comparative investigation on temperature distribution in electric discharge machining process through analytical, numerical and experimental methods”. Int. J. Mach. Tools Manuf, 114, 2017, pp. 35-53.
17. E. Weing¨artner, F. Kuster and K. Wegener. “Modeling and simulation of electrical discharge machining”. Procedia CIRP 2, 2012, pp.74– 78.
18. X. Bai, Q.H. Zhang, T.Y. Yang, J.H. Zhang. “Research on material removal rate of powder mixed near dry electrical discharge machining”. Int J Adv Manuf Technol, 2013.
19. B. Kuriachen, J. Mathew, “Spark Radius Modeling of Resistance-Capacitance Pulse Discharge in Micro-Electric Discharge Machining of Ti-6Al-4V: An Experimental Study”. Int. J. Adv. Manuf. Technol., Vol. 85(9–12), 2016, pp. 1983–1993.
20. Y. Sarikavak and C. Cogun, “Single discharge thermo-electrical modeling of micromachining mechanism in electric discharge machining”. Journal of Mechanical Science and Technology; Vol.26 (5), 2012, pp. 1591-1597.
21. P.T. Eubank, M.R. Patel, M.A. Barrufet and B. Bozkurt, “Theoretical models of the electrical discharge machining process. Part III: The variable mass, cylindrical plasma model”. J Appl Phys, Vol.73 (11), 1993, pp. 7900-7909.
22. T. Wang, J. Zhe, Y.Q. Zhang, Y.L. Li and X.R. Wen. “Thermal and fluid field simulation of single pulse discharge in dry EDM”, The Seventeenth CIRP Conference on Electro Physical and Chemical Machining (ISEM), Procedia CIRP,6 , 2013, pp. 427 – 431.

23. Y.H. Zhao, M. Kunieda and K. Abe, “EDM mechanism of single crystal SiC with respect to thermal, mechanical and chemical aspects”. J. Mater. Process. Technol., Vol.236, 2016, pp. 138-147
24. H. Hocheng, W.T. Lei and H.H. Hsu, “Preliminary study of material removal in electrical-discharge machining of SiC/Al”, J. Mater. Process. Technol., Vol.63, 1997, pp. 813-818
25. M. Shabgard, S.N.B. Oliaei, M. Seyedzavvar and A. Najadebrahimi, “Experimental investigation and 3D finite element prediction of the white layer thickness, heat affected zone, and surface roughness in EDM process”. J Mech Sci Technol, Vol.25 (12), 2011, pp. 3173-3183.
26. M. H. Kalajahi, S. R. Ahmadi and S.N.B Oliaei, “Experimental and finite element analysis of EDM process and investigation of material removal rate by response surface methodology”, Int. J. Adv. Manuf. Technol. 66, (2013),pp. 1–18.
27. S. Hinduja and M. Kunieda, “Modelling of ECM and EDM Processes”. CIRP Annals – Manufacturing Technology Vol.62(2), 2013, pp. 775–797.
28. B. Shao,“Modeling and simulation of micro elelctrical discharge machining”, University of Nebraska-Lincoln, 2015.
29. B.C. Xie, Y.K. Wang, Z.L Wang and W.S Zhao, “Numerical simulation of titanium alloy machining in electric discharge machining process”, Trans Nonferrous Metals Soc China, Vol.21, 2011, pp. 434–439
30. N.B. Salah, F. Ghanem and K.B. Atig, “Numerical study of thermal aspects of electric discharge machining process”, Int. J. Machine Tools Manufact., Vol.46 (7–8), 2006, pp. 908-911.
31. Saeed Assarzadeh and Majid Ghoreishi, “Electro-thermal-based finite element simulation and experimental validation of material removal in static gap single spark die-sinking electro-discharge machining process”. J Engineering Manufacture Vol.20, 2015, pp. 1-20.
32. Liu, J. F. and Guo, Y. B., “ Thermal Modeling of EDM With Progression of Massive Random Electrical Discharges,” 44th SME North American Manufacturing Research Conference (NAMRC), Blacksburg, VA, June 27–July 1, Vol. 5, 2016, pp. 495–507.
33. K. Oßwald, S. Schneider, L. Hensgen, A. Klink and F. Klocke, “Experimental investigation of energy distribution in continuous sinking

EDM", CIRP Journal of Manufacturing Science and Technology (in press), 2017.

34. A. Erden and B. Kaftanoglu, "Heat transfer modelling of electric discharge machining", in: 21st MTDR Conference, Swansea, 1980, pp. 351–358.
35. S.N. Joshi and S.S. Pande, "Development of an intelligent process model for EDM", International Journal of Advance Manufacturing Technology, Vol.45 (3), 2009, pp. 300-317
36. A. Tlili, F. Ghanem and N.B. Salah, "A contribution in EDM simulation field", International Journal of Advanced Manufacturing Technology, Vol.79, 2015, pp. 921-935.
37. Vijaykumar S. Jatti and Shivraj Bagane, "Thermo-electric modelling, simulation and experimental validation of powder mixed electric discharge machining (PMEDM) of BeCu alloys", Alexandria Engineering Journal, 2017.
38. Y. Zhang, Y. Liu, Y. Shen, Z. Li, R. Ji and F. Wang, "A new method of investigation the characteristic of the heat flux of EDM plasma Process", CIRP, Vol.6, 2013, pp. 451-456.
39. P. Shankar, V.K. Jain and T. Sundararajan, "Analysis of spark profiles during EDM process", Machinery Science & Technology, Vol.1 (2), 1997, pp. 195-217.
40. M.L. Jeswani, "Effect of the addition of graphite powder to kerosene used as the dielectric fluid in electrical discharge machining", Wear, Vol 70, 1981, pp. 133–139.
41. M. Kunieda, M. Yoshida and N. Taniguchi, "Electrical discharge machining in gas", Ann. CIRP, Vol. 46 (1), 1996, pp.143–146.
42. H. Marashi, MJ. Davoud, AAD. Sarhana, M. Hamdi, "State of the art in powder mixed dielectric for EDM applications". Precise Eng. Vol.46, 2016, pp.11–33.
43. M.P. Jahan, M. Rehman and Y.S. Wong. "Micro-electrical discharge machining (Micro-EDM)", Comprehensive Materials Processing, Elsevier, Oxford, 2014, pp. 333-371.
44. S. Chakraborty, V. Dey and S. K Ghosh, "A review on the use of dielectric fluids and their effects in electrical discharge machining characteristics", Precision Engineering, 2014.

45. Y. Shen, Y. Liu, W. Sun, Y. Zhang, H. Dong, C. Zheng and R. Ji, “High-speed near dry electrical discharge machining”. Journal of Material Processing Technology Vol.233, 2016, pp. 9–18.
46. Ou Shih-Fu and Wang Cong-Yu, “Effects of bio-ceramic particles in dielectric of powder-mixed electrical discharge machining on machining and surface characteristics of titanium alloys”. Vol.17 (17),2016, pp.30071-7.
47. K. Salonitis, A. Stournaras, P. Stavropoulos and G. Chryssolouris, “Thermal modeling of the material removal rate and surface roughness for die-sinking”, EDM International Journal of Advanced Manufacturing Technology, Vol.40, 2009, pp. 316-323.
48. P. Govindan, A. Gupta, S. S.Joshi, A. Malshe, and K. P Rajurkar, “Single-spark analysis of removal phenomenon in magnetic field assisted dry EDM”, J. Mater. Process. Technol., Vol.213 (7), 2013, pp. 1048-1058.
49. Ali Ahsan, Role of heat transfer on process characteristics during electrical discharge machining, Developments in Heat Transfer , 2009, pp. 417–435.
50. ANSYS manuals version 10.0. ANSYS TM Inc. USA.
51. H.P. Schulze, R. Herms, H. Juhr, W. Schaetzing and G. Wollenberg, “Comparison of measured and simulated crater morphology for EDM”, In: 14th International Symposium on Electro machining (ISEM XIV) Journal of Materials Processing Technology, Edinburgh, Scotland, UK 30 Mar. to 1 Apr. 2004, Elsevier 149, pp. 316–322.
52. J.V. Beck. “Transient temperatures in a semi-infinite cylinder heated by a disk heat source”, International Journal of Heat & Mass Transfer, Vol.24 (10), 1981, pp. 1631-1640.
53. P. C. Pandey and H. S. Shan, “Modern machining processes”, Tata McGraw-Hill, Chapter 5, 1980, pp. 7–38.
54. P. Fonda, Zhigang, Wang, Kazuo, Yamazaki. & A. Yuji, “A fundamental study on Ti-6Al-4V’s thermal and electrical properties and their relation to EDM productivity”. Journal of Materials Processing Technology, Vol.202, 2007, pp. 583-589.
55. F.L. Amorim, W.L. Weingaertner and I.A. Bassani, “Aspects on the optimization of die-sinking EDM of tungsten carbide-cobalt”, Journal of the Brazil Society of mechanical science & engineering, Vol.32, 2010, pp. 496-502.

56. J.W. Jung, Y.H. Jeong, B.K. Min and S.J. Lee. “Model-based Pulse Frequency Control for Micro-EDM Milling using Real-time Discharge Pulse Monitoring Journal of Manufacturing Science and Engineering”, Vol.130 (3), 2008, pp. 1-11.